


Full-state information–disturbance tradeoff for direction estimation with antiparallel spin-coherent pairs

Massimiliano F. Sacchi ^{1,2}

¹*CNR-Istituto di Fotonica e Nanotecnologie, Piazza Leonardo da Vinci 32, I-20133, Milano, Italy*

²*Dipartimento di Fisica, Università degli Studi di Pavia, Via Agostino Bassi 6, I-27100, Pavia, Italy*

We determine the optimal information–disturbance tradeoff for estimating an unknown spatial direction encoded in two antiparallel spins. Rotational covariance reduces the optimization over all instruments to a finite-dimensional Choi problem: a positive seed operator obeys one trace constraint for each irreducible sector of the input representation, while both the directional score and the operation fidelity are linear functionals of this seed. For two antiparallel spin-1/2 particles, whose physical representation decomposes as $0 \oplus 1$, we derive the two-multiplier dual problem and characterize the optimal instrument from the kernel vectors of the dual slack operator. The optimal operation is a covariant filter with scalar–vector coherence and is generally not a convex interpolation between the identity channel and a measure-and-reprepare strategy. At maximum information we recover the Gisin–Popescu score, but the least disturbing output state is optimized independently, giving a smaller disturbance than both the parallel-spin benchmark and antiparallel measure-and-reprepare. We also formulate the parallel benchmark and, as a central extension of the method, treat antiparallel spin-coherent states of arbitrary spin j . In this case the signal coherently occupies all sectors $\ell = 0, \dots, 2j$ of $j \otimes j$, the endpoint information is governed by nearest-neighbor sector coherences, and the endpoint disturbance is obtained from an explicit finite block-diagonal eigenvalue problem.

I. INTRODUCTION

A quantum measurement has two inseparable roles. It produces classical information about the system, but it also implements a physical operation on the postmeasurement state. In general these two roles are in tension: a more informative measurement causes a larger back action on the state left for subsequent use. This tension, already present in the early discussion of measurement disturbance [1], is commonly quantified through information–disturbance tradeoffs. Such tradeoffs have been studied for state discrimination and estimation, weak and partial measurements, continuous variables, and reversible or approximately reversible measurement schemes [2–16]. Here we consider a geometric version of the problem: the unknown parameter is a spatial direction encoded in a pair of spins.

Direction estimation is a natural setting for covariant quantum estimation. Alice chooses a unit vector uniformly on the sphere and prepares a state in the corresponding group orbit. Bob applies an instrument whose outcome gives a guess for the direction and whose conditional output is the state that remains after the measurement. We quantify the information by the standard directional score $s(\vec{n}, \vec{m}) = (1 + \vec{n} \cdot \vec{m})/2$, where \vec{m} is the true direction and \vec{n} is the guess [17–23]. We quantify the disturbance by $D = 1 - F$, where F is the full-state operation fidelity between the input pure state of the complete two-spin signal and the conditional output. Thus the identity channel has $D = 0$, while an informative measurement generally has $D > 0$. Because F depends on the output state and not only on the measurement probabilities, optimizing the disturbance requires optimizing the full instrument.

A related information–disturbance problem for antiparallel spin-1/2 direction transmission was considered in Ref. [24]. There, however, the disturbance functional was marginal: it tested the survival of one output spin through an observable of the form $|\psi_g\rangle\langle\psi_g| \otimes I$. In the present work we use the full-state operation fidelity of the complete two-spin signal. This changes the operational problem: the zero-disturbance point is the identity operation with random directional score $I = 1/2$, rather than the marginal zero-disturbance point $I = 2/3$. The two analyses are therefore operationally distinct.

The physical comparison motivating the paper is between parallel and antiparallel encodings. In both cases the physical rotation acting on the two spins is the same, namely $V_g = U_g \otimes U_g$, where U_g denotes an irreducible representation of the rotation g . The distinction between the two encodings is the choice of fiducial state. For two spin-1/2 the parallel pair is generated from $|\uparrow\rangle|\uparrow\rangle$ and is confined to the symmetric spin-one sector. The antiparallel pair is generated from $|\uparrow\rangle|\downarrow\rangle$ and has coherent components in both the singlet and triplet sectors, i.e. in the decomposition $1/2 \otimes 1/2 \simeq 0 \oplus 1$. This sector coherence is the relevant resource for direction estimation.

The role of collective measurements in extracting information from multipartite quantum systems was already highlighted by Peres and Wootters [25]. In the present direction-estimation setting, Gisin and Popescu showed that two antiparallel spin-1/2 particles can carry more directional information than two parallel ones when collective measurements are allowed [21]. The advantage is not due to entanglement of the signal state, which is a product state, but to the coherent occupation of inequivalent irreducible sectors. Related developments include optimal

reference-frame transmission, covariant maximum-likelihood measurements, group-transformation estimation, photonic orienteering experiments, and recent work on incompatibility and device estimation with parallel and antiparallel spins [26–32].

The question addressed here is whether the antiparallel advantage survives when measurement back action is included. At the fully informative endpoint for two spin-1/2 particles we find that it does: the antiparallel encoding gives a larger information score and a smaller minimum disturbance than the parallel encoding. Moreover, the least disturbing endpoint operation is not the naive measure-and-reprepare channel that prepares the guessed antiparallel state. At fixed optimal measurement, the output state remains a variational degree of freedom; optimizing it reduces the disturbance below both the parallel endpoint value and the antiparallel measure-and-reprepare value. This separation between optimal statistics and optimal postmeasurement state is analogous to what occurs in state-discrimination tradeoffs [11]. The advantage of antiparallel encoding survives along the entire optimal information–disturbance tradeoff curve.

The main technical tool used in this paper is covariance. Since the prior, the signal ensemble, and the score are rotationally invariant, any strategy can be group averaged without changing the averaged information or operation fidelity. The optimization can therefore be restricted to covariant instruments. In the Jamiolkowski representation a covariant instrument is described by one positive seed Choi operator. Trace preservation gives one linear constraint for each irreducible sector of the input representation, and both figures of merit are linear functionals of the seed. The tradeoff boundary is therefore a semidefinite optimization problem with a simple representation-theoretic structure [33–35]. We use the standard formalism of quantum operations, instruments, covariant measurements, and Choi–Jamiolkowski operators [29, 36–44]. The same framework is closely related to earlier uses of covariance, vectorization, and group representation theory in Bell measurements, optimal realizations of positive maps, maximum-likelihood estimation, and information–disturbance tradeoffs [10–12, 45, 46]. For two antiparallel spin-1/2 particles the supporting-line optimization has two trace multipliers. We derive the corresponding dual slack operator and characterize the optimal seed by its kernel. For generic interior points this kernel is one-dimensional, giving a rank-one covariant filter with scalar–vector mixing. This mixing is precisely the structure that exploits the coherence between inequivalent angular-momentum sectors and explains why the optimal tradeoff is not a convex interpolation between the identity channel and a measure-and-reprepare strategy. We also derive endpoint formulas for antiparallel spin-coherent states of arbitrary spin j , in a setting closely related to optimal spin-direction encoding and decoding [22, 47]. In this case the representation decomposes as $j \otimes j \simeq \bigoplus_{\ell=0}^{2j} \ell$, and the fiducial antiparallel state has coherent amplitudes in all sectors. The maximum information is controlled by nearest-neighbor coherences between sectors ℓ and $\ell + 1$, while the minimum endpoint disturbance is the largest eigenvalue of an explicit finite block-diagonal operator. This sector structure is related to the broader role of finite reference frames, covariance, and approximate symmetry constraints in quantum information processing and error correction [48–56]. This arbitrary-spin endpoint analysis is more than a formal generalization: it shows that the same covariance-and-kernel-vector method organizes the tradeoff for an increasing number of irreducible sectors, replacing the two-sector spin-1/2 problem by a controlled finite family of sector constraints and block eigenvalue problems.

The paper is organized as follows. Section II introduces quantum instruments, the information and disturbance figures of merit, and the covariant Jamiolkowski reduction. Sections III and IV solve the antiparallel spin-1/2 problem from the covariant dual, while Sec. V discusses the endpoints and the improvement over measure-and-reprepare. Section VI gives the irreducible parallel-spin benchmark. The extension to arbitrary antiparallel spin is formulated in Sec. VII, and the maximum-information endpoint for arbitrary spin is evaluated in Sec. VIII. Appendix A briefly relates the present full-state disturbance to the marginal-disturbance tradeoff of Ref. [24]. Appendix B contains the fixed-POVM output optimization used at the endpoints. Appendices C and D collect the rank statements for optimal Choi seeds: the one-dimensional-kernel criterion for rank-one optimality and the general convex-geometric low-rank bound. Appendix E derives the large-spin asymptotics of the antiparallel endpoint problem.

II. COVARIANT FORMULATION

A. Instruments and figures of merit

A measurement with outcome r is described by a quantum instrument, namely a collection of trace-decreasing completely positive maps [36, 38, 41],

$$\mathcal{E}_r(\rho) = \sum_{\mu} A_{r\mu} \rho A_{r\mu}^{\dagger}. \quad (1)$$

For a discrete outcome set, the probability of outcome r on an input state ρ is $p_r = \text{Tr}[\mathcal{E}_r(\rho)] = \text{Tr}[\Pi_r \rho]$, and, when $p_r > 0$, the conditional output state is $\rho_r = \mathcal{E}_r(\rho)/p_r$. The associated POVM is

$$\Pi_r = \sum_{\mu} A_{r\mu}^{\dagger} A_{r\mu}, \quad \sum_r \Pi_r = I_{\text{in}}, \quad (2)$$

where I_{in} denotes the identity operator in the input Hilbert space. The completeness relation is equivalent to trace preservation of the nonselective operation $\sum_r \mathcal{E}_r$.

In the direction-estimation problem the outcomes are continuous and are identified with unit vectors \vec{n} on the sphere. We use the normalized invariant measure $\int d\vec{n} = 1$, so that

$$\int d\vec{n} \sum_{\mu} A_{\vec{n}\mu}^{\dagger} A_{\vec{n}\mu} = I_{\text{in}}. \quad (3)$$

All probabilities below are therefore probability densities with respect to $d\vec{n}$.

Let the signal states form a covariant orbit

$$|\psi_g\rangle = V_g |\psi_0\rangle, \quad g \in G, \quad (4)$$

where G is compact and the prior is the normalized Haar measure. In the applications below $G = \text{SU}(2)$, or equivalently $\text{SO}(3)$ for the orbit of directions, and the fiducial state is associated with the reference direction \vec{z} . Although we often write group elements g , the physical outcome is the direction $\vec{n} = g\vec{z}$, namely the coset $gH \in \text{SU}(2)/\text{U}(1)$; all outcome integrals are normalized sphere integrals unless explicitly stated otherwise. Throughout the paper, V_g denotes the physical representation acting on the spin system under consideration. For a pair of physical spin- j particles this means $V_g = U_g^{(j)} \otimes U_g^{(j)}$, where $U_g^{(j)}$ is the spin- j irreducible representation of the rotation g .

For a true reference direction \vec{z} , the information extracted by the instrument is defined as the average score

$$I = \int d\vec{n} \sum_{\mu} s(n_z) \langle \psi_z | A_{\vec{n}\mu}^{\dagger} A_{\vec{n}\mu} | \psi_z \rangle, \quad (5)$$

where $s(n_z) = (1 + n_z)/2$. This is the standard directional score used in covariant estimation of a spatial direction [17, 18, 21]. For a true direction \vec{m} and a guessed direction \vec{n} , more generally $s(\vec{n}, \vec{m}) = (1 + \vec{n} \cdot \vec{m})/2 = \cos^2(\theta/2)$, where θ is the angle between the two directions. The score is normalized between zero and one, gives unit score for a correct guess, zero score for the opposite direction, and Haar average 1/2 for a random guess. For spin-one-half coherent states it coincides with the transition probability between the two pure states whose Bloch vectors are \vec{n} and \vec{m} . We use the same score for all spin values because the estimated parameter is the spatial direction itself.

The disturbance is one minus the operation fidelity,

$$D = 1 - F, \quad F = \int d\vec{n} \sum_{\mu} |\langle \psi_z | A_{\vec{n}\mu} | \psi_z \rangle|^2. \quad (6)$$

For later use it is helpful to spell out how Eq. (6) is obtained from the conditional states. If the input is the pure state $\rho_z = |\psi_z\rangle\langle\psi_z|$, the probability density of the outcome \vec{n} is

$$p(\vec{n}|z) = \sum_{\mu} \langle \psi_z | A_{\vec{n}\mu}^{\dagger} A_{\vec{n}\mu} | \psi_z \rangle. \quad (7)$$

The corresponding conditional output is

$$\rho_{\vec{n}|z} = \frac{1}{p(\vec{n}|z)} \sum_{\mu} A_{\vec{n}\mu} \rho_z A_{\vec{n}\mu}^{\dagger}. \quad (8)$$

The contribution of this outcome to the average state survival is therefore

$$p(\vec{n}|z) \langle \psi_z | \rho_{\vec{n}|z} | \psi_z \rangle = \sum_{\mu} |\langle \psi_z | A_{\vec{n}\mu} | \psi_z \rangle|^2. \quad (9)$$

Integrating over the outcomes gives F in Eq. (6). This derivation also shows why the disturbance is sensitive not only to the POVM elements $A_{\vec{n}\mu}^{\dagger} A_{\vec{n}\mu}$, but to the particular Kraus realization of the instrument: different postmeasurement states can have the same statistics and different operation fidelities. For pure input states this is the average overlap between the original state and the conditional postmeasurement state, weighted by the outcome probability. We refer to Eq. (6) as a full-state operation fidelity to distinguish it from marginal disturbance functionals that probe only part of the output system; see Appendix A. With this convention, the identity operation gives $D = 0$ and an uninformative guess gives $I = 1/2$.

B. Covariant reduction

The use of covariance is standard in quantum statistical decision theory and in the theory of covariant instruments [17, 36–40, 44]. Suppose that an arbitrary instrument $\{\mathcal{E}_r\}$ is used with a guess rule $r \mapsto g_r$. Define the covariantized instrument

$$\tilde{\mathcal{E}}_h(\rho) = \sum_r V_h V_{g_r}^\dagger \mathcal{E}_r \left(V_{g_r} V_h^\dagger \rho V_h V_{g_r}^\dagger \right) V_{g_r} V_h^\dagger. \quad (10)$$

The equality of the averaged figures of merit before and after covariantization follows directly from invariance. For example, the information of the original strategy can be written as

$$I = \int dg \sum_r s(g_r, g) \text{Tr}[\mathcal{E}_r(V_g \rho_0 V_g^\dagger)]. \quad (11)$$

Inserting Eq. (10), changing variables by left and right Haar invariance, and using $s(kg_r, kg) = s(g_r, g)$ leaves this integral unchanged. The same calculation applies to the operation fidelity because both the input projector and the output projector are rotated by the same unitary. Hence covariance is not an ansatz: it is a consequence of group averaging together with linearity of the figures of merit. Because both I and F are linear in the instrument before the final optimization, the group average of an arbitrary strategy preserves the averaged values; no convexity or extremality assumption is involved at this stage. For a continuous outcome set the sum is replaced by the corresponding integral. Thus no optimality is lost by restricting the search to covariant instruments.

A covariant instrument satisfies

$$\mathcal{E}_h(V_g \rho V_g^\dagger) = V_g \mathcal{E}_{g^{-1}h}(\rho) V_g^\dagger. \quad (12)$$

Equivalently, all maps are generated from a single seed map \mathcal{E}_0 ,

$$\mathcal{E}_g(\rho) = V_g \mathcal{E}_0(V_g^\dagger \rho V_g) V_g^\dagger. \quad (13)$$

For direction estimation the physical outcome is not a full rotation but a point on the sphere, $S^2 \simeq G/H$, where the stabilizer subgroup $H \simeq U(1)$ consists of rotations around the fiducial direction \vec{z} . If g and gh , with $h \in H$, send \vec{z} to the same direction, they correspond to the same guess. Moreover, the score depends only on the coset gH .

The fiducial signal states used below are invariant under the stabilizer at the level relevant for the figures of merit. For parallel spin-coherent states, rotations around \vec{z} produce only an overall phase. For the antiparallel fiducial state $|j, j\rangle|j, -j\rangle$, the two phases produced by a rotation around \vec{z} are opposite and cancel. Thus the projector $|\psi_z\rangle\langle\psi_z|$ is invariant under H . The seed instrument may therefore be averaged over the stabilizer without changing I or F . With the normalized decomposition $dg = d\vec{n} dh$, this removes the redundant rotation around the guessed direction and leaves a covariant instrument labeled only by $\vec{n} \in S^2$.

C. Jamiołkowski representation and SDP form

We use the Jamiołkowski representation of completely positive maps [42]. Together with the covariance reduction above, this gives the standard finite-dimensional form of a covariant-instrument optimization problem [36, 37, 40, 44]. For a completely positive seed map \mathcal{E}_0 we define

$$R_0 = (I_{\text{in}} \otimes \mathcal{E}_0)|\Phi\rangle\langle\Phi|, \quad |\Phi\rangle = \sum_i |i\rangle|i\rangle, \quad (14)$$

so that

$$\mathcal{E}_0(\rho) = \text{Tr}_{\text{in}}[(\rho^\tau \otimes I_{\text{out}})R_0], \quad R_0 \geq 0. \quad (15)$$

Here τ denotes transposition in the basis used to define the unnormalized maximally entangled vector $|\Phi\rangle$. We also use the double-ket notation for vectorization [45]. If $X = \sum_{ij} X_{ij} |i\rangle_{\text{out}} \langle j|_{\text{in}}$ is a linear operator from the input Hilbert space to the output Hilbert space, then

$$|X\rangle\rangle = \sum_{ij} X_{ij} |j\rangle_{\text{in}} |i\rangle_{\text{out}}, \quad \langle\langle X|Y \otimes Z|X\rangle\rangle = \text{Tr}[X^\dagger ZXY^\tau]. \quad (16)$$

With this convention a rank-one Choi operator $R = |X\rangle\rangle\langle\langle X|$ represents the single-Kraus map $E(\rho) = X\rho X^\dagger$. The Choi operator for outcome g is

$$R_g = (V_g^* \otimes V_g) R_0 (V_g^\tau \otimes V_g^\dagger), \quad (17)$$

and trace preservation of the nonselective operation is equivalent to

$$\int dg V_g^* \text{Tr}_{\text{out}}[R_0] V_g^\tau = I_{\text{in}}. \quad (18)$$

To obtain the trace constraint explicitly, insert Eq. (15) in the condition that the nonselective map is trace preserving. For the seed one has

$$\text{Tr}[\mathcal{E}_0(\rho)] = \text{Tr}[(\rho^\tau \otimes I_{\text{out}}) R_0] = \text{Tr}[\rho^\tau \text{Tr}_{\text{out}} R_0]. \quad (19)$$

For the covariant family one averages the input-side operator $Y = \text{Tr}_{\text{out}} R_0$ over the representation V_g^* , which is the action induced by the transposition convention in the Choi representation, giving Eq. (18). In general the input representation may contain multiplicities [17, 28, 44]:

$$V_g^* \simeq \bigoplus_{\alpha} \left(U_g^{(\alpha)} \otimes I_{m_{\alpha}} \right), \quad (20)$$

where $U_g^{(\alpha)}$ acts on the irrep space and $I_{m_{\alpha}}$ is the identity on the multiplicity space. Schur's lemma then averages over the irrep factor and leaves an operator on the multiplicity factor. In the representations treated explicitly in this work, namely $0 \oplus 1$ and $\bigoplus_{\ell=0}^{2j} \ell$, each irrep occurs once, so $m_{\alpha} = 1$ and the condition reduces to one scalar trace constraint per sector. Equivalent irreducible components would lead instead to matrix-valued constraints on the multiplicity spaces and cannot be ignored in general [57]. The two quantities of interest are affine-linear functions of the seed:

$$I = \text{Tr}(R_I R_0), \quad D = 1 - \text{Tr}(R_F R_0). \quad (21)$$

The positive operators R_I and R_F are obtained by the group averages

$$R_I = \int dg s(g) (V_g |\psi_0\rangle\langle\psi_0| V_g^\dagger)^\tau \otimes I_{\text{out}}. \quad (22)$$

$$R_F = \int dg (V_g |\psi_0\rangle\langle\psi_0| V_g^\dagger)^\tau \otimes V_g |\psi_0\rangle\langle\psi_0| V_g^\dagger, \quad (23)$$

The operators R_I and R_F are obtained by moving all dependence on the seed map into R_0 . For instance, with $\rho_g = V_g |\psi_0\rangle\langle\psi_0| V_g^\dagger$,

$$\text{Tr}[\mathcal{E}_g(\rho_g)] = \text{Tr}[(\rho_g^\tau \otimes I) R_g] \quad (24)$$

and covariance allows the group action to be shifted from R_g to the fixed seed. Averaging the resulting coefficient of R_0 gives Eq. (22). Similarly,

$$\langle\psi_g | \mathcal{E}_g(\rho_g) | \psi_g\rangle = \text{Tr}[(\rho_g^\tau \otimes \rho_g) R_g], \quad (25)$$

which gives Eq. (23) after the same change of variables. Thus the primal optimization is linear in the Choi seed. Here $s(g)$ is the directional score associated with the direction obtained by applying g to the fiducial direction. Thus, at fixed information, the minimum-disturbance problem is the SDP

$$\begin{aligned} & \text{minimize} && 1 - \text{Tr}(R_F R_0) \\ & \text{subject to} && R_0 \geq 0, \\ & && \text{Tr}(R_I R_0) = I, \\ & && \int dg V_g^* \text{Tr}_{\text{out}}[R_0] V_g^\tau = I_{\text{in}}. \end{aligned} \quad (26)$$

The following sections solve this program explicitly for the two spin-one-half encodings and derive closed endpoint formulas for arbitrary spin.

III. TWO ANTIPARALLEL SPIN-ONE-HALF PARTICLES

A. Representation and signal states

The physical antiparallel pair is

$$|\psi_{\vec{n}}\rangle = |\vec{n}\rangle|-\vec{n}\rangle = (U_g \otimes U_g)|\uparrow\rangle|\downarrow\rangle, \quad \vec{n} = g\vec{z}. \quad (27)$$

The two-spin Hilbert space decomposes as

$$\frac{1}{2} \otimes \frac{1}{2} \simeq 0 \oplus 1. \quad (28)$$

We introduce the singlet–triplet Cartesian basis

$$\{|0\rangle, |x\rangle, |y\rangle, |z\rangle\}, \quad (29)$$

where

$$|0\rangle = \frac{1}{\sqrt{2}}(|\uparrow\downarrow\rangle - |\downarrow\uparrow\rangle) \quad (30)$$

spans the scalar sector, while $|x\rangle, |y\rangle, |z\rangle$ span the triplet sector and are chosen as a real Cartesian vector basis. In particular,

$$|z\rangle = \frac{1}{\sqrt{2}}(|\uparrow\downarrow\rangle + |\downarrow\uparrow\rangle), \quad (31)$$

with phases of $|x\rangle$ and $|y\rangle$ chosen so that

$$(U_g \otimes U_g)|z\rangle = n_x|x\rangle + n_y|y\rangle + n_z|z\rangle. \quad (32)$$

Since

$$|\uparrow\rangle|\downarrow\rangle = \frac{1}{\sqrt{2}}(|0\rangle + |z\rangle), \quad (33)$$

the antiparallel signal associated with the unit vector \vec{n} is

$$|\psi_{\vec{n}}\rangle = \frac{1}{\sqrt{2}}(|0\rangle + n_x|x\rangle + n_y|y\rangle + n_z|z\rangle), \quad (34)$$

and the fiducial state is

$$|\psi_z\rangle = \frac{1}{\sqrt{2}}(|0\rangle + |z\rangle). \quad (35)$$

The simple scalar-plus-vector form is therefore obtained directly in the physical $U_g \otimes U_g$ representation. It is the singlet–triplet analogue of the operator identity $|\vec{n}\rangle\langle\vec{n}| = (I + \vec{n} \cdot \vec{\sigma})/2$, but it is written entirely in the physical two-spin Hilbert space. The scalar–vector coherence in Eq. (34) is the resource responsible for the antiparallel advantage in direction estimation [21].

We use the normalized invariant measure on the sphere,

$$\int d\vec{n} = 1, \quad \int d\vec{n} n_i = 0, \quad \int d\vec{n} n_i n_j = \frac{\delta_{ij}}{3}. \quad (36)$$

The optimal covariant direction POVM has density

$$\Pi_{\vec{n}} = |\eta_{\vec{n}}\rangle\langle\eta_{\vec{n}}|, \quad |\eta_{\vec{n}}\rangle = |0\rangle + \sqrt{3}(n_x|x\rangle + n_y|y\rangle + n_z|z\rangle). \quad (37)$$

Indeed, Eq. (36) gives

$$\int d\vec{n} \Pi_{\vec{n}} = P_0 + P_1 = I_{\text{in}}, \quad P_0 = |0\rangle\langle 0|, \quad P_1 = I_{\text{in}} - P_0. \quad (38)$$

For a true z direction, with $x = n_z$, the likelihood of this POVM is

$$p_{\text{opt}}(x) = |\langle\eta_{\vec{n}}|\psi_z\rangle|^2 = \frac{1}{2}(1 + \sqrt{3}x)^2. \quad (39)$$

With the directional score $s(x) = (1 + x)/2$, this gives the Gisin–Popescu value [21]

$$I_{\text{max}} = \int_{-1}^1 \frac{dx}{2} \frac{1+x}{2} \frac{1}{2} (1 + \sqrt{3}x)^2 = \frac{3 + \sqrt{3}}{6}. \quad (40)$$

B. Seed of the covariant instrument

As explained after Eq. (19) trace preservation of the nonselective operation gives one constraint per irreducible sector. More explicitly, if $Y = \text{Tr}_{\text{out}} R_0$, Eq. (18) gives

$$\int dg V_g^* Y V_g^\tau = \frac{\text{Tr}(P_0 Y P_0)}{1} P_0 + \frac{\text{Tr}(P_1 Y P_1)}{3} P_1. \quad (41)$$

Equating this expression to $P_0 + P_1 = I_{\text{in}}$ yields

$$\text{Tr}[P_0 \text{Tr}_{\text{out}}(R_0) P_0] = 1, \quad \text{Tr}[P_1 \text{Tr}_{\text{out}}(R_0) P_1] = 3. \quad (42)$$

These numbers are simply the dimensions of the irreducible sectors. Equivalently, with

$$A_0 = P_0 \otimes I_4, \quad A_1 = P_1 \otimes I_4, \quad (43)$$

we write

$$\text{Tr}(A_0 R_0) = 1, \quad \text{Tr}(A_1 R_0) = 3. \quad (44)$$

The information and operation fidelity are linear functions of R_0 :

$$I = \text{Tr}(R_I R_0), \quad F = \text{Tr}(R_F R_0), \quad D = 1 - F. \quad (45)$$

In the ordered basis of Eq. (29) on the input factor $R_I = B_I \otimes I_4$, where

$$B_I = \begin{pmatrix} \frac{1}{4} & 0 & 0 & \frac{1}{12} \\ 0 & \frac{1}{12} & 0 & 0 \\ 0 & 0 & \frac{1}{12} & 0 \\ \frac{1}{12} & 0 & 0 & \frac{1}{12} \end{pmatrix}. \quad (46)$$

Equation (46) can be checked directly. Since $|\psi_{\vec{n}}\rangle = (|0\rangle + n_i|i\rangle)/\sqrt{2}$ and $s(n_z) = (1 + n_z)/2$, the input coefficient is

$$B_I = \frac{1}{4} \int d\vec{n} (1 + n_z) (|0\rangle + n_i|i\rangle) (\langle 0| + n_j\langle j|). \quad (47)$$

The required moments are those in Eq. (36); for example, $\langle 0|B_I|0\rangle = 1/4$, $\langle 0|B_I|z\rangle = (1/4) \int d\vec{n} n_z^2 = 1/12$, and $\langle i|B_I|j\rangle = (1/4)\delta_{ij}/3$. All other entries vanish by parity or axial symmetry. The operator R_F is given by

$$R_F = \int d\vec{n} |\psi_{\vec{n}}\rangle \langle \psi_{\vec{n}}|^\tau \otimes |\psi_{\vec{n}}\rangle \langle \psi_{\vec{n}}|. \quad (48)$$

Its matrix elements are $(R_F)_{ab,cd} = M_{abcd}/4$, where $a, b, c, d \in \{0, x, y, z\}$ and the nonzero components are

$$\begin{aligned} M_{0000} &= 1, \\ M_{00ij} &= M_{0i0j} = M_{0ij0} = M_{i00j} = M_{i0j0} = M_{ij00} = \frac{\delta_{ij}}{3}, \\ M_{ijkl} &= \frac{\delta_{ij}\delta_{kl} + \delta_{ik}\delta_{jl} + \delta_{il}\delta_{jk}}{15}. \end{aligned} \quad (49)$$

Rotational invariance fixes all nonzero components. Terms containing an odd number of vector indices vanish by inversion symmetry. Terms with two vector indices give $\int d\vec{n} n_i n_j = \delta_{ij}/3$. Terms with four vector indices give the unique isotropic rank-four tensor

$$\int d\vec{n} n_i n_j n_k n_l = a(\delta_{ij}\delta_{kl} + \delta_{ik}\delta_{jl} + \delta_{il}\delta_{jk}). \quad (50)$$

Contracting $i = j$ and $k = l$ yields $1 = \int d\vec{n} (\vec{n} \cdot \vec{n})^2 = 15a$, hence $a = 1/15$. Thus M_{abcd} is the component form of the group average in Eq. (48), turning the abstract covariant expression for R_F into an explicit finite matrix for the SDP.

IV. OPTIMAL TRADEOFF FROM THE COVARIANT DUAL PROBLEM

To trace the boundary of the achievable region we maximize a supporting linear functional of the operation fidelity and the information. For a fixed real parameter μ this amounts to maximizing

$$F + \mu I = \text{Tr}[(R_F + \mu R_I)R_0]. \quad (51)$$

Varying μ gives the supporting lines of the concave optimal curve $F(I)$, or equivalently of the convex disturbance curve $D(I) = 1 - F(I)$. For an irreducible input representation there is only one trace constraint, and the optimization reduces to a largest-eigenvalue problem. In the antiparallel spin-1/2 case the input representation is $0 \oplus 1$, and the two sector normalizations lead to

$$\begin{aligned} & \text{minimize} && \lambda_0 + 3\lambda_1 \\ & \text{subject to} && K_\mu(\lambda_0, \lambda_1) = \lambda_0 A_0 + \lambda_1 A_1 - (R_F + \mu R_I) \geq 0. \end{aligned} \quad (52)$$

This dual follows from the Lagrangian of the primal maximization of $\text{Tr}[(R_F + \mu R_I)R_0]$ under $\text{Tr}(A_0 R_0) = 1$, $\text{Tr}(A_1 R_0) = 3$, and $R_0 \geq 0$:

$$\mathcal{L}(R_0, \lambda_0, \lambda_1) = \lambda_0 + 3\lambda_1 - \text{Tr}[(\lambda_0 A_0 + \lambda_1 A_1 - R_F - \mu R_I) R_0]. \quad (53)$$

The Lagrangian is bounded above over $R_0 \geq 0$ iff the operator in parentheses is positive. At optimality, complementary slackness gives [33]

$$K_\mu(\lambda_0, \lambda_1) R_0^* = 0, \quad (54)$$

so the support of every optimal Choi seed is contained in the zero eigenspace of the optimal dual slack.

For the antiparallel spin-1/2 problem the active kernel of the dual slack is one-dimensional along the generic interior branch. Let $|X_\mu\rangle\rangle$ be the corresponding normalized kernel vector. The sector constraints read

$$\langle\langle X_\mu | A_0 | X_\mu \rangle\rangle = \frac{1}{4}, \quad \langle\langle X_\mu | A_1 | X_\mu \rangle\rangle = \frac{3}{4}, \quad (55)$$

and the optimal seed is

$$R_0(\mu) = 4 |X_\mu\rangle\rangle \langle\langle X_\mu|. \quad (56)$$

Appendix C gives the general reason for this normalization: when the active kernel of the dual slack is one-dimensional, the KKT conditions force its sector weights to be proportional to the sector dimensions.

This rank-one construction describes the generic exposed branch. At endpoints or isolated values of μ the active kernel may be degenerate. If $\ker K_\mu = \text{span}\{|X_1\rangle\rangle, \dots, |X_d\rangle\rangle\}$, complementary slackness gives only $\text{supp } R_0^* \subseteq \ker K_\mu$. The most general optimal seed on that exposed face is

$$R_0^* = \sum_{r,s=1}^d G_{rs} |X_r\rangle\rangle \langle\langle X_s|, \quad G \geq 0, \quad (57)$$

where G is chosen to satisfy

$$\sum_{r,s} G_{rs} \langle\langle X_s | A_0 | X_r \rangle\rangle = 1, \quad \sum_{r,s} G_{rs} \langle\langle X_s | A_1 | X_r \rangle\rangle = 3. \quad (58)$$

Thus a degenerate active kernel leaves only a reduced finite-dimensional SDP inside the exposed face; a diagonal mixture is sufficient only when the sector normalizations can be met without coherences among the kernel vectors.

In the simple-kernel case,

$$I(\mu) = 4 \langle\langle X_\mu | R_I | X_\mu \rangle\rangle, \quad F(\mu) = 4 \langle\langle X_\mu | R_F | X_\mu \rangle\rangle, \quad D(\mu) = 1 - F(\mu). \quad (59)$$

Axial symmetry around the fiducial direction allows the seed Kraus operator to be chosen real and of the form

$$X_\mu = \begin{pmatrix} u_\mu & 0 & 0 & v_\mu \\ 0 & w_\mu & 0 & 0 \\ 0 & 0 & w_\mu & 0 \\ r_\mu & 0 & 0 & s_\mu \end{pmatrix}. \quad (60)$$

The corresponding covariant instrument is

$$\mathcal{E}_{\vec{n}}^{(\mu)}(\rho) = A_{\vec{n}}^{(\mu)} \rho A_{\vec{n}}^{(\mu)\dagger}, \quad A_{\vec{n}}^{(\mu)} = 2V_g X_\mu V_g^\dagger, \quad \vec{n} = g\vec{z}. \quad (61)$$

The scalar–vector mixing terms v_μ and r_μ are the operational signature of the coherence between inequivalent irreducible sectors. They also show why the optimal curve is not, in general, obtained by convexly interpolating between the identity channel and a measure-and-reprepare map.

For every feasible R_0 ,

$$\text{Tr}[(R_F + \mu R_I)R_0] \leq \lambda_0(\mu) + 3\lambda_1(\mu), \quad (62)$$

and equality is attained by Eq. (56) in the simple-kernel case, or by any feasible seed of Eq. (57) in a degenerate case. Hence Eq. (59) generates the globally optimal covariant tradeoff.

V. ENDPOINTS AND COMPARISON WITH MEASURE-AND-REPREPARE

At $\mu = 0$ the linear objective is just F . Trivially, the optimal instrument is the identity channel and

$$I(0) = \frac{1}{2}, \quad F(0) = 1, \quad D(0) = 0. \quad (63)$$

The opposite endpoint is obtained as $\mu \rightarrow \infty$, where the information is maximized first. The optimal POVM is Eq. (37), but the output state need not be the guessed signal state. At this endpoint the seed Kraus operator has the rank-one form

$$X_\infty = \frac{1}{2}|\varphi_z\rangle\langle\eta_z|, \quad |\varphi_z\rangle = \cos\beta|0\rangle + \sin\beta|z\rangle. \quad (64)$$

The operation fidelity is obtained by applying the fixed-POVM output optimization of Appendix B to the optimal POVM. The maximum-information likelihood is

$$|\langle\eta_{\vec{n}}|\psi_z\rangle|^2 = \frac{1}{2}(1 + \sqrt{3}n_z)^2. \quad (65)$$

Thus the remaining output-state optimization is governed by

$$Q = \int d\vec{n} |\langle\eta_{\vec{n}}|\psi_z\rangle|^2 V_g^\dagger |\psi_z\rangle\langle\psi_z| V_g, \quad \vec{n} = g\vec{z}. \quad (66)$$

Since the likelihood and the fiducial input are invariant under rotations around z , Q commutes with the stabilizer of z . Hence the relevant maximizing output vector belongs to $\text{span}\{|0\rangle, |z\rangle\}$, and the transverse states $|x\rangle, |y\rangle$ do not contribute to the largest eigenvalue. Direct evaluation of the spherical moments gives

$$Q|_{\{0,z\}} = \begin{pmatrix} \frac{1}{2} & \frac{\sqrt{3}}{6} \\ \frac{\sqrt{3}}{6} & \frac{7}{30} \end{pmatrix}. \quad (67)$$

The diagonal entries are the likelihood-weighted survival contributions of the scalar and longitudinal output components, while the off-diagonal entry is the corresponding scalar–longitudinal coherence. The largest eigenvector fixes the best fiducial output state $|\varphi_z\rangle$, and the largest eigenvalue is the endpoint operation fidelity. The eigenvalues are

$$q_\pm = \frac{11 \pm \sqrt{91}}{30}, \quad (68)$$

so the maximum operation fidelity, i.e. the largest eigenvalue of Q , is

$$F(I_{\max}) = \frac{11 + \sqrt{91}}{30}, \quad (69)$$

and therefore the minimal disturbance is

$$D(I_{\max}) = 1 - \lambda_{\max}(Q) = \frac{19 - \sqrt{91}}{30} \simeq 0.31535. \quad (70)$$

The angle β in Eq. (64) is fixed by the normalized eigenvector of Q associated with this largest eigenvalue. This shows explicitly that the optimal output is a covariant family generated from a state in the scalar-longitudinal subspace, rather than being imposed a priori to coincide with the guessed signal state. The disturbance in Eq. (70) is smaller than the disturbance of the measure-and-reprepare endpoint, where the output state is forced to be the guessed signal state $|\psi_{\vec{n}}\rangle$. In that case

$$F_{\text{mr}}(I_{\text{max}}) = \int_{-1}^1 \frac{dx}{2} \frac{1}{2} (1 + \sqrt{3}x)^2 \left(\frac{1+x}{2} \right)^2 = \frac{11 + \sqrt{75}}{30}, \quad (71)$$

and therefore

$$D_{\text{mr}}(I_{\text{max}}) = \frac{19 - \sqrt{75}}{30} \simeq 0.34466. \quad (72)$$

Thus, even at maximal information, minimum disturbance requires optimizing the postmeasurement state, not merely repreparing the guessed signal state. A similar result appeared also at the endpoint of the optimal information-disturbance tradeoff in quantum-state discrimination [11].

VI. PARALLEL-SPIN BENCHMARK

The parallel two-spin benchmark is useful because it is the irreducible version of the same optimization problem. Two parallel spin-one-half particles occupy the symmetric subspace and are equivalent to a single spin coherent state with total spin $J = 1$. We denote the coherent state in this subspace by

$$|\phi_{\vec{n}}\rangle = U_g^{(J)} |J, J\rangle, \quad \vec{n} = g\vec{z}. \quad (73)$$

The representation is irreducible. Therefore, unlike the antiparallel case, there is a single trace-preserving constraint for the covariant Choi seed,

$$\text{Tr } R_0 = 2J + 1 = 3. \quad (74)$$

This irreducibility makes the benchmark technically simpler: optimizing a linear combination of information and operation fidelity reduces to a maximum-eigenvalue problem rather than to a semidefinite problem with several sector multipliers.

For the directional score used throughout this paper, the two linear operators are

$$R_I^{\parallel} = \int d\vec{n} \frac{1 + n_z}{2} |\phi_{\vec{n}}\rangle \langle \phi_{\vec{n}}|^{\tau} \otimes I_{J=1}, \quad (75)$$

$$R_F^{\parallel} = \int d\vec{n} |\phi_{\vec{n}}\rangle \langle \phi_{\vec{n}}|^{\tau} \otimes |\phi_{\vec{n}}\rangle \langle \phi_{\vec{n}}|. \quad (76)$$

For each real parameter μ one defines

$$C_{\mu}^{\parallel} = R_F^{\parallel} + \mu R_I^{\parallel}. \quad (77)$$

Since the normalization constraint is only $\text{Tr } R_0 = 3$, the dual slack is

$$K_{\mu}^{\parallel} = \lambda I_3 \otimes I_3 - C_{\mu}^{\parallel}, \quad (78)$$

and the smallest feasible λ is the largest eigenvalue of C_{μ}^{\parallel} . Hence, if

$$C_{\mu}^{\parallel} |\chi_{\mu}\rangle\rangle = c_{\text{max}}(\mu) |\chi_{\mu}\rangle\rangle, \quad \langle\langle \chi_{\mu} | \chi_{\mu} \rangle\rangle = 1, \quad (79)$$

then the optimal Choi seed is

$$R_0^{\parallel}(\mu) = 3 |\chi_{\mu}\rangle\rangle \langle\langle \chi_{\mu} |. \quad (80)$$

The corresponding optimal benchmark curve is

$$I^{\parallel}(\mu) = 3 \langle\langle \chi_{\mu} | R_I^{\parallel} | \chi_{\mu} \rangle\rangle, \quad D^{\parallel}(\mu) = 1 - 3 \langle\langle \chi_{\mu} | R_F^{\parallel} | \chi_{\mu} \rangle\rangle. \quad (81)$$

Equivalently, writing the eigenvector in vectorized form as the Kraus seed χ_μ , the optimal covariant instrument has the form

$$\mathcal{E}_g^\parallel(\rho) = 3U_g^{(J)}\chi_\mu U_g^{(J)\dagger} \rho U_g^{(J)}\chi_\mu^\dagger U_g^{(J)\dagger}. \quad (82)$$

This is the irreducible counterpart of the dual-kernel construction used for antiparallel spins. In the antiparallel case the scalar and vector sectors force two multipliers λ_0, λ_1 ; in the parallel case the single multiplier λ is just the largest eigenvalue of C_μ^\parallel .

At the fully informative endpoint the coherent-state POVM in the spin- J subspace has density [12, 59, 60]

$$\Pi_{\vec{n}}^\parallel = (2J + 1)|\phi_{\vec{n}}\rangle\langle\phi_{\vec{n}}|. \quad (83)$$

For a true z direction,

$$|\langle\phi_{\vec{n}}|\phi_z\rangle|^2 = \left(\frac{1+x}{2}\right)^{2J}, \quad x = n_z, \quad (84)$$

and hence, for $J = 1$, the endpoint information is

$$I_{\max}^\parallel = \int_{-1}^1 \frac{dx}{2} \frac{1+x}{2} 3 \left(\frac{1+x}{2}\right)^2 = \frac{3}{4}. \quad (85)$$

At the same endpoint, the POVM is fixed but the output state is not. Using Appendix B, the residual optimization is described by

$$Q^\parallel = 3 \int d\vec{n} |\langle\phi_{\vec{n}}|\phi_z\rangle|^2 U_g^{(J)\dagger} |\phi_z\rangle\langle\phi_z| U_g^{(J)}. \quad (86)$$

For any fiducial output $|\varphi_z\rangle$ in the spin- J space,

$$F(\varphi) = \langle\varphi_z|Q^\parallel|\varphi_z\rangle. \quad (87)$$

Axial symmetry makes Q^\parallel diagonal in the J_z basis: the weight $|\langle\phi_{\vec{n}}|\phi_z\rangle|^2$ depends only on n_z , so the azimuthal integral removes all matrix elements with different magnetic quantum numbers. For $J = 1$ its eigenvalues are

$$q_1 = \frac{3}{5}, \quad q_0 = \frac{3}{10}, \quad q_{-1} = \frac{1}{10}. \quad (88)$$

Thus the maximum is obtained by repreparing the guessed coherent state itself, and

$$F(I_{\max}^\parallel) = \frac{3}{5}, \quad D(I_{\max}^\parallel) = 1 - \frac{3}{5} = \frac{2}{5}. \quad (89)$$

The endpoint comparison with the optimized antiparallel construction is then

$$I_{\max}^{\text{anti}} = \frac{3 + \sqrt{3}}{6} > \frac{3}{4} = I_{\max}^\parallel, \quad (90)$$

while

$$D(I_{\max}^{\text{anti}}) = \frac{19 - \sqrt{91}}{30} < \frac{2}{5} = D(I_{\max}^\parallel). \quad (91)$$

Thus the antiparallel encoding remains advantageous even with respect to the figure of merit of disturbance. The complete comparison of the optimal information-disturbance tradeoffs for the two spin-1/2 case is shown in Fig. 1.

A global quantity that in both cases continuously characterizes the covariant instruments that optimize the information-disturbance tradeoff is the normalized squared trace of the Kraus seeds X_μ and χ_μ in Eqs. (61) and (82), respectively. Expressed as a function of the extracted information, for antiparallel encoding the scalar $t(I) = |\text{Tr } X(I)|^2/4$ equals 1 at the identity endpoint, where no information is extracted beyond the random score $I = 1/2$, and decreases concavely to $|\text{Tr } X(I_{\max})|^2/4 = (\cos\beta + \sqrt{3}\sin\beta)^2/16 \simeq 0.19707$ at the maximum-information endpoint, where $|\varphi_z\rangle = \cos\beta|0\rangle + \sin\beta|z\rangle$ is the largest-eigenvalue eigenvector of the endpoint operator Q in Eq. (67). For the parallel case $t(I^\parallel) = |\text{Tr } \chi(I^\parallel)|^2/3$ equals 1 at the identity endpoint and $1/3$ at the maximum-information value $I_{\max}^\parallel = 3/4$. We plot the results of $t(I)$ for both cases in Fig. 2.

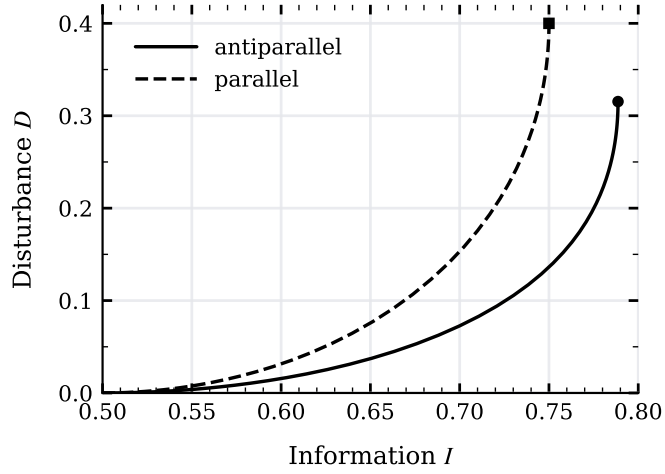


FIG. 1. Optimal information–disturbance tradeoffs for two-spin direction encoding. The solid curve is the antiparallel spin-1/2 case obtained from the two-sector dual-kernel construction. The dashed curve is the parallel-spin benchmark, equivalent to the irreducible spin- $J = 1$ spin-coherent-state problem. The markers denote the fully informative endpoints.

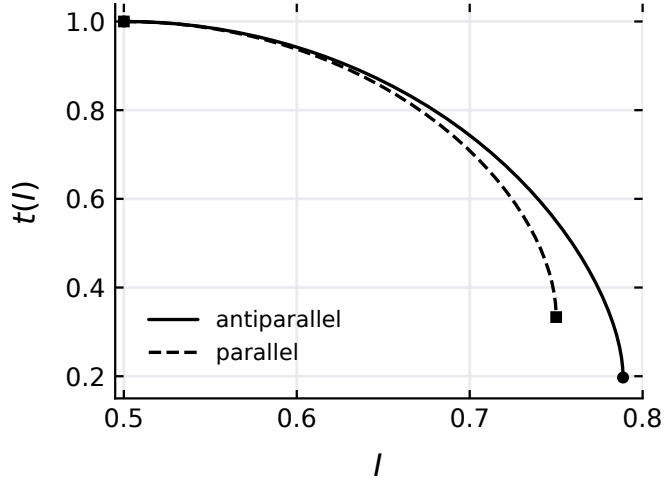


FIG. 2. Normalized squared traces of the Kraus seeds along the optimal tradeoffs for two spin-1/2 particles. The solid curve is the antiparallel encoding, with $t(I) = |\text{Tr } X(I)|^2/4$; the dashed curve is the parallel encoding, with $t(I^\parallel) = |\text{Tr } \chi(I^\parallel)|^2/3$.

VII. HIGHER-SPIN ANTIPARALLEL STATES

Here we extend our study to antiparallel spin-coherent states of arbitrary spin j ,

$$|\psi_{\vec{n}}^{(j)}\rangle = |\vec{n}\rangle_j |-\vec{n}\rangle_j = (U_g^{(j)} \otimes U_g^{(j)})|j, j\rangle|j, -j\rangle, \quad \vec{n} = g\vec{z}. \quad (92)$$

The representation is the ordinary two-spin representation

$$V_g^{(j)} = U_g^{(j)} \otimes U_g^{(j)}, \quad (93)$$

and it decomposes as

$$j \otimes j \simeq \bigoplus_{\ell=0}^{2j} \ell. \quad (94)$$

The fiducial state decomposes as [61]

$$|j, j\rangle|j, -j\rangle = \sum_{\ell=0}^{2j} c_{\ell} |\ell, 0\rangle, \quad c_{\ell}^2 = (2\ell + 1) \frac{[(2j)!]^2}{(2j - \ell)!(2j + \ell + 1)!}. \quad (95)$$

The coefficients in Eq. (95) are the Clebsch–Gordan coefficients

$$c_{\ell} = \langle j, j; j, -j | \ell, 0 \rangle, \quad (96)$$

up to an overall phase, chosen here so that all c_{ℓ} are nonnegative. Normalization follows from completeness of the coupled basis, $\sum_{\ell=0}^{2j} c_{\ell}^2 = 1$. The factorial expression shows that all sectors allowed by angular-momentum addition appear, so the fiducial antiparallel signal is not confined to a single irreducible representation. The optimal POVM seed for direction estimation is $|\eta_z^{(j)}\rangle\langle\eta_z^{(j)}|$, with

$$|\eta_z^{(j)}\rangle = \sum_{\ell=0}^{2j} \sqrt{2\ell + 1} |\ell, 0\rangle. \quad (97)$$

The normalization of the POVM seed follows from the orthogonality relation for irreducible matrix elements. In fact, in the sector ℓ , the orbit of $|\ell, 0\rangle$ satisfies

$$\int d\vec{n} U_g^{(\ell)} |\ell, 0\rangle \langle\ell, 0| U_g^{(\ell)\dagger} = \frac{\Delta_{\ell}}{2\ell + 1}, \quad (98)$$

where Δ_{ℓ} denotes the projectors onto the irreducible sectors, while cross terms between inequivalent irreducible sectors average to zero. Therefore the integral of $|\eta_{\vec{n}}^{(j)}\rangle\langle\eta_{\vec{n}}^{(j)}|$ is $\sum_{\ell} \Delta_{\ell} = I_{\text{in}}$. Defining

$$A_{\ell} = \Delta_{\ell} \otimes I_{\text{out}}, \quad (99)$$

the trace constraints are

$$\text{Tr}(A_{\ell} R_0) = 2\ell + 1, \quad \ell = 0, 1, \dots, 2j. \quad (100)$$

The supporting-line optimization is therefore

$$\begin{aligned} & \text{minimize} \quad \sum_{\ell=0}^{2j} (2\ell + 1) \lambda_{\ell} \\ & \text{subject to} \quad K_{\mu}^{(j)} = \sum_{\ell=0}^{2j} \lambda_{\ell} A_{\ell} - (R_F^{(j)} + \mu R_I^{(j)}) \geq 0. \end{aligned} \quad (101)$$

The optimal Choi seed is supported on the kernel of $K_{\mu}^{(j)}$. This is the higher-spin analogue of the irreducible maximum-eigenvector construction, but with $2j + 1$ trace multipliers replacing the single multiplier of an irreducible representation.

Although the dual kernel can be multidimensional, the general rank-reduction argument of Appendix D shows that there always exists an optimal covariant Choi seed with $\text{rank } R_0^* \leq \lfloor \sqrt{2j + 1} \rfloor$. Hence the $j = 1$ antiparallel tradeoff admits a rank-one optimal seed.

The optimal information–disturbance tradeoff for the case of two spins $j = 1$ is represented in Fig. 3, where the comparison with the case of parallel encoding is also reported.

VIII. ENDPOINT INFORMATION AND DISTURBANCE FOR ARBITRARY SPIN

We now collect the endpoint quantities for two spin- j coherent states, both for antiparallel and parallel encodings. The endpoint considered here is the fully informative endpoint: the covariant POVM is chosen to maximize the directional information, and, once this POVM is fixed, the output state is chosen so as to maximize the operation fidelity. This is important because the minimum-disturbing endpoint need not coincide with a measure-and-reprepare channel in which the guessed signal state itself is reprepared.

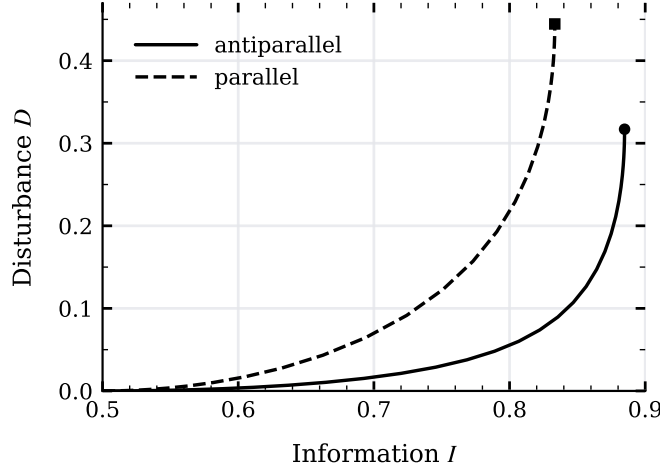


FIG. 3. Optimal information–disturbance tradeoffs for two-spin direction encoding with $j = 1$. The solid curve is the antiparallel encoding, obtained from the three-sector dual-kernel construction for $1 \otimes 1 \simeq 0 \oplus 1 \oplus 2$. The dashed curve is the parallel encoding, equivalent to the irreducible spin- $J = 2$ spin-coherent-state problem. The markers denote the fully informative endpoints.

A. Antiparallel encoding

Using the POVM seed of Eq. (97) for direction estimation and defining

$$\alpha_\ell = \sqrt{2\ell + 1} c_\ell, \quad (102)$$

we can write the maximum-information likelihood for a state with relative angle θ , with $x = n_z = \cos \theta$, as

$$p_j(x) = \left| \langle \eta_{\vec{n}}^{(j)} | \psi_z^{(j)} \rangle \right|^2 = T_j(x)^2, \quad (103)$$

where

$$T_j(x) = \sum_{\ell=0}^{2j} \alpha_\ell P_\ell(x) \quad (104)$$

is given in terms of the Legendre polynomials $P_\ell(x)$, since the matrix element of a rotated $m = 0$ vector is $\langle \ell, 0 | U_g^{(\ell)} | \ell, 0 \rangle = P_\ell(\cos \theta)$ [61]. The maximum information is then

$$I_{\max}^{\text{anti},j} = \int_{-1}^1 \frac{dx}{2} \frac{1+x}{2} T_j(x)^2. \quad (105)$$

Using the Legendre orthogonality and recurrence relations [62]

$$\int_{-1}^1 \frac{dx}{2} P_\ell(x) P_{\ell'}(x) = \frac{\delta_{\ell\ell'}}{2\ell + 1}, \quad (106)$$

$$x P_\ell(x) = \frac{\ell + 1}{2\ell + 1} P_{\ell+1}(x) + \frac{\ell}{2\ell + 1} P_{\ell-1}(x), \quad (107)$$

one obtains

$$I_{\max}^{\text{anti},j} = \frac{1}{2} + \sum_{\ell=0}^{2j-1} \frac{\ell + 1}{\sqrt{(2\ell + 1)(2\ell + 3)}} c_\ell c_{\ell+1}. \quad (108)$$

Since multiplication by x connects P_ℓ only to $P_{\ell+1}$ and $P_{\ell-1}$, only coherences between adjacent irreducible sectors enter the information gain above a random guess. Equivalently, substituting Eq. (95) gives

$$I_{\max}^{\text{anti},j} = \frac{1}{2} + \sum_{\ell=0}^{2j-1} (\ell + 1) \frac{[(2j)!]^2}{\sqrt{(2j - \ell)!(2j + \ell + 1)!(2j - \ell - 1)!(2j + \ell + 2)!}}. \quad (109)$$

We now optimize the endpoint disturbance. At maximum information the POVM is fixed by Eq. (97), but the output state after each outcome is still a variational degree of freedom. Applying the fixed-POVM construction of Appendix B, with likelihood $T_j(n_z)^2$, gives the positive operator

$$Q_j = \int d\vec{n} T_j(n_z)^2 V_g^\dagger |\psi_z^{(j)}\rangle \langle \psi_z^{(j)}| V_g, \quad \vec{n} = g\vec{z}. \quad (110)$$

For a covariant output generated by a fiducial vector $|\varphi_z\rangle$ in $\bigoplus_{\ell=0}^{2j} \mathcal{H}_\ell$, the endpoint fidelity is

$$F^{\text{anti},j}(\varphi) = \langle \varphi_z | Q_j | \varphi_z \rangle. \quad (111)$$

Thus

$$F(I_{\text{max}}^{\text{anti},j}) = \lambda_{\text{max}}(Q_j), \quad D(I_{\text{max}}^{\text{anti},j}) = 1 - \lambda_{\text{max}}(Q_j). \quad (112)$$

Because $T_j(x)^2$ is invariant under rotations around the z axis, Q_j is block diagonal in the magnetic quantum number m . We denote by $d_{m0}^\ell(\theta)$ the reduced Wigner rotation matrix element in the sector of total angular momentum ℓ . As shown in Appendix B2, in the coupled basis $|\ell, m\rangle$, the block with fixed m has matrix elements

$$\left[Q_j^{(m)} \right]_{\ell\ell'} = c_\ell c_{\ell'} \int_{-1}^1 \frac{dx}{2} T_j(x)^2 d_{m0}^\ell(\theta) d_{m0}^{\ell'}(\theta), \quad (113)$$

where $x = \cos \theta$ and $\ell, \ell' = |m|, |m| + 1, \dots, 2j$. Therefore

$$F(I_{\text{max}}^{\text{anti},j}) = \max_m \lambda_{\text{max}}(Q_j^{(m)}), \quad D(I_{\text{max}}^{\text{anti},j}) = 1 - \max_m \lambda_{\text{max}}(Q_j^{(m)}). \quad (114)$$

The symmetry $m \leftrightarrow -m$ allows one to restrict the maximization to $m \geq 0$.

For $j = 1/2$, the matrix in Eq. (113) contains an $m = 0$ block and one-dimensional $|m| = 1$ blocks; the largest eigenvalue belongs to the $m = 0$ block and gives Eq. (67). For higher spin, all numerical calculations reported below give the largest eigenvalue in the $m = 0$ block. We have not found a general analytic proof that this must hold for every j : although Q_j is positive and block diagonal in m , the block kernels contain reduced Wigner functions $d_{m0}^\ell(\theta)$, whose signs and relative magnitudes do not imply a simple ordering of the block norms as $|m|$ increases. We therefore retain the rigorous maximization over m in Eq. (114); the statement that $m = 0$ is the maximizing block is reported as numerical evidence for the values in Table I up to $j = 5$.

B. Parallel encoding

Two parallel spin- j coherent states are supported in the maximal total-spin sector and are equivalent to a single spin coherent state with total spin $J = 2j$. From Eqs. (83) and (84), the likelihood at the fully informative endpoint is

$$p_J(x) = (2J + 1) \left(\frac{1+x}{2} \right)^{2J}. \quad (115)$$

The endpoint information is then

$$I_{\text{max}}^{\parallel,j} = \int_{-1}^1 \frac{dx}{2} \frac{1+x}{2} p_J(x) = \frac{2J+1}{2J+2} = \frac{4j+1}{4j+2}. \quad (116)$$

At the same endpoint, the output state is optimized after the maximum-information coherent-state POVM has been fixed. Appendix B gives

$$Q_J^\parallel = (2J + 1) \int d\vec{n} |\langle \phi_{\vec{n}} | \phi_z \rangle|^2 U_g^{(J)\dagger} |J, J\rangle \langle J, J| U_g^{(J)}, \quad \vec{n} = g\vec{z}. \quad (117)$$

For a fiducial output $|\varphi_z\rangle$,

$$F_{\text{max } I}^{\parallel,j}(\varphi) = \langle \varphi_z | Q_J^\parallel | \varphi_z \rangle. \quad (118)$$

TABLE I. Endpoint information and disturbance for antiparallel and parallel spin-coherent encodings. The antiparallel disturbance is obtained by optimizing the output state after the maximum-information POVM, i.e. from Eq. (114) after maximizing over all magnetic-number blocks. For all displayed values the maximizing block is the $m = 0$ block.

j	I_{\max}^{anti}	$D(I_{\max}^{\text{anti}})$	I_{\max}^{\parallel}	$D(I_{\max}^{\parallel})$
1/2	0.788675	0.315354	0.750000	0.400000
1	0.884773	0.316957	0.833333	0.444444
3/2	0.923549	0.311796	0.875000	0.461538
2	0.942636	0.309422	0.900000	0.470588
5/2	0.953792	0.308743	0.916667	0.476190
3	0.961168	0.308782	0.928571	0.480000
7/2	0.966456	0.309074	0.937500	0.482759
4	0.970455	0.309428	0.944444	0.484848
9/2	0.973593	0.309770	0.950000	0.486486
5	0.976125	0.310081	0.954545	0.487805

As shown in Appendix B 3, Q_j^{\parallel} is diagonal in the J_z basis, its diagonal entries increase with m , and therefore its largest eigenvalue occurs at $m = J$. Hence the optimal endpoint output is the guessed coherent state itself, and the corresponding endpoint operation fidelity is

$$F(I_{\max}^{\parallel,j}) = (2J + 1) \int_{-1}^1 \frac{dx}{2} \left(\frac{1+x}{2} \right)^{4J} = \frac{2J+1}{4J+1}. \quad (119)$$

Therefore

$$D(I_{\max}^{\parallel,j}) = 1 - F(I_{\max}^{\parallel,j}) = \frac{2J}{4J+1} = \frac{4j}{8j+1}. \quad (120)$$

C. Endpoint comparison

The parallel endpoint has closed formulas (116) and (120). The antiparallel maximum information is given by Eq. (108), while the corresponding minimum disturbance is obtained from the finite eigenvalue problem in Eq. (114).

Both endpoint information values approach unity as j increases. The endpoint disturbances, however, behave differently. For parallel spins,

$$D(I_{\max}^{\parallel,j}) = \frac{4j}{8j+1} \longrightarrow \frac{1}{2}. \quad (121)$$

For antiparallel spins the finite-matrix calculation gives a disturbance close to 0.31 over the range shown in Table I, well below the corresponding parallel value. Thus, at the fully informative endpoint, the antiparallel encoding gives both larger directional information and smaller disturbance. The corresponding values of Table I are also reported in Fig. 4. The antiparallel endpoint disturbance is not strictly monotone in j . It has a shallow minimum around $j = 5/2$ in the range displayed, and then slowly increases, remaining close to 0.31 and well below the parallel endpoint disturbance. Thus the relevant robust conclusion is not monotonicity, but the persistent separation between the antiparallel and parallel endpoint disturbances.

The large- j limit of the antiparallel endpoint disturbance can also be obtained analytically. As shown in Appendix E one has

$$\lim_{j \rightarrow \infty} D(I_{\max}^{\text{anti},j}) = 8\sqrt{2} - 11 \simeq 0.313708. \quad (122)$$

The shallow minimum observed at finite j is therefore not the asymptotic value, but a finite-spin effect.

Remark on the full tradeoff for higher spin. The endpoint formulas are simpler than the full tradeoff because the maximum-information POVM is fixed and only the output state remains to be optimized; the disturbance then follows from the finite eigenvalue problem in Eq. (114). Away from the endpoint one must optimize the full covariant Choi seed. For antiparallel spin j the dual problem in Eq. (101) contains $2j + 1$ sector multipliers, whereas the parallel spin-coherent benchmark is irreducible and has only one trace constraint.

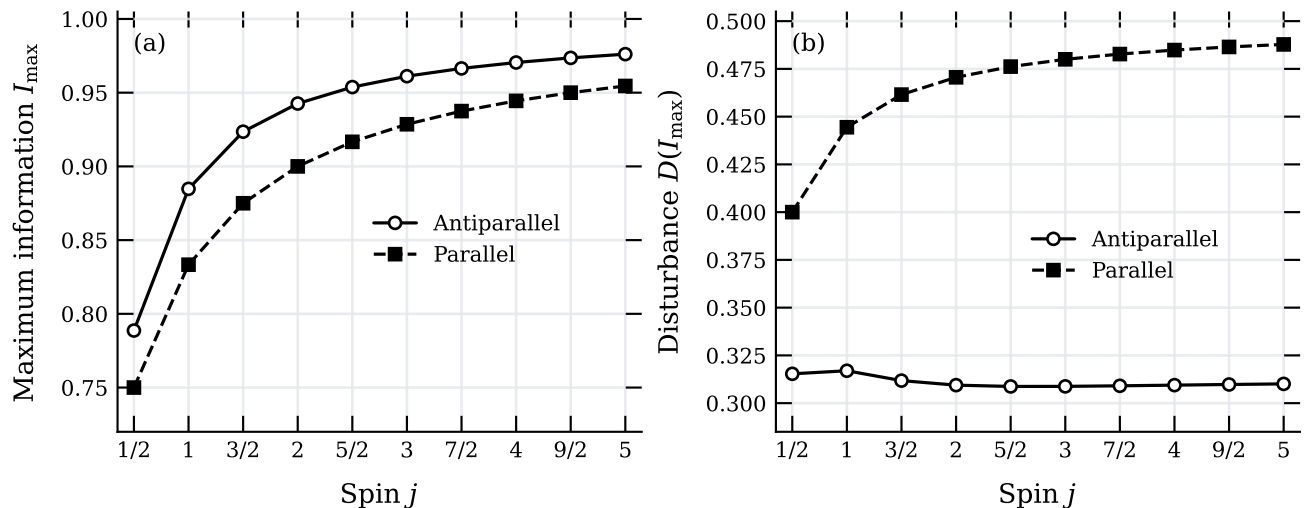


FIG. 4. Endpoint comparison for antiparallel and parallel spin-coherent encodings as a function of the spin j . Solid curves with circles denote the antiparallel encoding, and dashed curves with squares denote the parallel encoding. Panel (a) shows the maximum directional information. Panel (b) shows the antiparallel endpoint disturbance obtained after optimizing the output state for the maximum-information POVM; it remains substantially below the parallel one. The antiparallel curve is not strictly monotone; it displays a shallow minimum at intermediate spin.

The rank structure of the optimal Choi seed is clarified in Appendices C and D. If the active kernel of the dual slack is one-dimensional, Appendix C shows that its sector weights are automatically correct and the optimal seed can be chosen rank one. Independently, Appendix D gives the general low-rank guarantee $\text{rank } R_0^* \leq \lfloor \sqrt{2j+1} \rfloor$. Thus rank one is forced by convex geometry for $j = 1/2$ and $j = 1$, while for higher spin it is a spectral property of the active dual kernel. If that kernel is genuinely degenerate, the optimal face is described by Eq. (57) with a positive matrix G satisfying all sector normalizations.

It is useful to distinguish the coherent-product comparison studied here from the ultimate direction-encoding problem with two spin- j systems. For $j > 1/2$, the state that maximizes the information over all pure two-spin states is generally entangled and is not the antiparallel spin-coherent product state. Equivalently, its amplitudes in the sectors $\ell = 0, \dots, 2j$ are not, in general, the Clebsch–Gordan coefficients in Eq. (95). For example, for two spin-one particles the information-optimal fiducial state is

$$|\psi_z^{\text{opt}}\rangle = \frac{\sqrt{10}}{6}|0,0\rangle + \frac{1}{\sqrt{2}}|1,0\rangle + \frac{\sqrt{2}}{3}|2,0\rangle, \quad (123)$$

which gives

$$I_{\text{opt}}^{(j=1)} = \frac{1}{2} + \frac{\sqrt{15}}{10} \simeq 0.887298. \quad (124)$$

The antiparallel spin-one coherent product state instead gives

$$I_{\text{max}}^{\text{anti},1} = \frac{1}{2} + \frac{\sqrt{5}}{15} + \frac{\sqrt{2}}{6} \simeq 0.884773. \quad (125)$$

The construction of information-optimal direction encodings can be obtained by following the general procedure discussed in Ref. [64]. In the present work, however, we deliberately compare two physically transparent separable encodings—parallel and antiparallel spin-coherent pairs—and optimize the measurement back action for those encodings. To our knowledge, the information–disturbance tradeoff for antiparallel spin- j coherent pairs, together with the corresponding endpoint comparison with parallel spin- j coherent pairs, has not been worked out previously.

IX. CONCLUSIONS

We have formulated the optimal information–disturbance tradeoff for the estimation of direction encoded in two spins as a covariant Jamiołkowski optimization problem. The construction separates the operational ingredients

from the representation theory. The operational ingredients are the information functional, defined by the average directional score, and the operation fidelity, defined by the average overlap between the input state and the conditional output state. The representation theory determines the trace constraints on the seed Choi operator: one independent constraint is obtained for each irreducible sector appearing in the input orbit.

For two antiparallel spin-one-half particles the relevant representation is $0 \oplus 1$. The optimal supporting-line problem therefore has two dual multipliers. We wrote the dual slack operator explicitly and showed that the optimal seed is supported on its zero eigenspace. For generic interior points of the spin-one-half curve this eigenspace is one-dimensional, giving a rank-one filter generated from the kernel vector; if the zero eigenspace is degenerate, the remaining task is the reduced positive feasibility problem within that kernel. The allowed filter has scalar–vector mixing, which is precisely the structure required to exploit the coherence responsible for the antiparallel advantage. This also shows why the optimal tradeoff is not generally obtained by simply interpolating between doing nothing and performing a measurement followed by reparation.

At the maximum-information endpoint the POVM is the optimal covariant orientation measurement. The output state, however, remains a variational parameter. Optimizing it gives the antiparallel spin-one-half disturbance, which is below both the disturbance of the corresponding measure-and-reprepare antiparallel strategy and the parallel-spin endpoint value. Thus, antiparallel spins are better in both senses: they provide more directional information and suffer less minimum disturbance.

The arbitrary-spin endpoint analysis shows how this advantage is organized for general spin-coherent signals. For antiparallel spin- j states the orbit decomposes as $j \otimes j = \bigoplus_{\ell=0}^{2j} \ell$. The maximum information contains only nearest-neighbor coherences between these sectors, while the corresponding minimum disturbance is the largest eigenvalue of an explicit finite block-diagonal operator. For the values reported, the antiparallel endpoint information exceeds the parallel value and the antiparallel endpoint disturbance remains substantially smaller than the parallel disturbance.

Away from the maximum-information endpoint, the full higher-spin problem is a genuine multiconstraint semidefinite program. The dual slack contains $2j + 1$ independent multipliers, and its kernel may have dimension larger than one; a feasible optimal Choi operator can then require a positive combination of several kernel projectors satisfying all sector normalizations. This kernel-feasibility problem is absent in irreducible parallel-spin benchmarks and is the main mathematical complication in the complete higher-spin tradeoff. The present formulation provides the natural starting point for such calculations and for analytic certificates of optimality in higher-dimensional cases.

Appendix A: Relation to a marginal-disturbance tradeoff for antiparallel spin-1/2 states

Reference [24] studies a related information–disturbance problem for antiparallel spin-1/2 direction transmission, motivated by eavesdropping on reference-frame communication. The main difference is the disturbance functional. In that work the disturbance tests the survival of one output spin, through a fidelity of the form

$$F_{\text{marg}} = \int dg \sum_{r\mu} \text{Tr} [A_{r\mu} \tilde{\rho}_g A_{r\mu}^\dagger (|\psi_g\rangle\langle\psi_g| \otimes I)]. \quad (\text{A1})$$

This is a marginal figure of merit: a measurement on the second spin can leave the tested first-spin state undisturbed. Consequently the zero-disturbance endpoint of that problem occurs at information $2/3$.

The present paper uses instead the full-state operation fidelity of the complete two-spin signal,

$$F_{\text{full}} = \int d\vec{n} \sum_{\mu} |\langle\psi_z|A_{\vec{n}\mu}|\psi_z\rangle|^2. \quad (\text{A2})$$

Here any nontrivial measurement on either spin generally disturbs the complete input state, and the zero-disturbance endpoint is the identity operation, with $I = 1/2$. Thus the two analyses are related but operationally distinct: Ref. [24] studies a marginal-disturbance tradeoff, whereas the present work studies the full-state operation-fidelity tradeoff of the complete two-spin signal. The comparison is mentioned here only to clarify the choice of disturbance functional; the optimization carried out in the main text concerns the full-state operation fidelity in Eq. (A2) and its natural extension to arbitrary spin j .

Appendix B: Endpoint output optimization at fixed covariant POVM

This appendix gives the fixed-POVM construction used in the endpoint calculations of the main text and writes it explicitly in terms of $SU(2)$ representation matrix elements. The setting is the fully informative endpoint: the covariant

POVM has already been chosen to maximize the directional information, and the only remaining variational freedom is the conditional output state.

1. General fixed-POVM construction

Let the fixed endpoint POVM be rank one and covariant, with seed $|\eta_z\rangle\langle\eta_z|$. For the outcome $\vec{n} = g\vec{z}$ we write

$$|\eta_{\vec{n}}\rangle = V_g|\eta_z\rangle. \quad (\text{B1})$$

At the endpoint, a covariant choice of pure output states is similarly generated from a single fiducial vector $|\varphi_z\rangle$,

$$|\varphi_{\vec{n}}\rangle = V_g|\varphi_z\rangle. \quad (\text{B2})$$

For a true input $|\psi_z\rangle$, define

$$\rho_z = |\psi_z\rangle\langle\psi_z|, \quad p(g|z) = p(\vec{n}|z) = |\langle\eta_{\vec{n}}|\psi_z\rangle|^2. \quad (\text{B3})$$

The endpoint operation fidelity at fixed POVM is

$$F(\varphi) = \int d\vec{n} p(\vec{n}|z) |\langle\psi_z|V_g|\varphi_z\rangle|^2 = \langle\varphi_z|Q|\varphi_z\rangle, \quad (\text{B4})$$

where

$$Q = \int d\vec{n} p(\vec{n}|z) V_g^\dagger \rho_z V_g. \quad (\text{B5})$$

Thus Q is the likelihood-weighted average of the true input projector, rotated back to the fiducial output frame. It does not determine the maximum-information POVM; that POVM is already fixed and gives information I_{\max} . Instead, Q solves the remaining output-state optimization. Since $Q \geq 0$,

$$F(I_{\max}) = \lambda_{\max}(Q), \quad D(I_{\max}) = 1 - \lambda_{\max}(Q), \quad (\text{B6})$$

and the optimal fiducial output state is any normalized eigenvector associated with $\lambda_{\max}(Q)$.

2. Antiparallel spin- j representation

We now derive the block formula used in Eq. (114). We use the coupled basis $|\ell, m\rangle$ and the Wigner-matrix convention [61]

$$U_g^{(\ell)}|\ell, m'\rangle = \sum_m D_{mm'}^{(\ell)}(g)|\ell, m\rangle. \quad (\text{B7})$$

The endpoint likelihood is the function $T_j(n_z)^2$ defined in Eqs. (103) and (104). Its dependence only on $n_z = \cos\theta$ follows from the identity

$$D_{00}^{(\ell)}(g) = d_{00}^\ell(\theta) = P_\ell(\cos\theta), \quad (\text{B8})$$

for the $m = 0$ matrix element [61].

Substituting the decomposition of Eq. (95) into Eq. (110) gives

$$\langle\ell, m|Q_j|\ell', m'\rangle = c_\ell c_{\ell'} \int d\vec{n} T_j(n_z)^2 D_{m0}^{(\ell)}(g^{-1}) D_{0m'}^{(\ell')}(g). \quad (\text{B9})$$

Writing g in Euler angles, the azimuthal integral enforces $m = m'$. Therefore Q_j is block diagonal in the magnetic quantum number,

$$Q_j = \bigoplus_m Q_j^{(m)}. \quad (\text{B10})$$

The block with fixed m has entries

$$[Q_j^{(m)}]_{\ell\ell'} = c_\ell c_{\ell'} \int_{-1}^1 \frac{dx}{2} T_j(x)^2 d_{m0}^\ell(\theta) d_{m0}^{\ell'}(\theta), \quad x = \cos\theta, \quad (\text{B11})$$

where $\ell, \ell' = |m|, |m| + 1, \dots, 2j$. Equation (114) follows by maximizing the largest eigenvalue over these finite blocks.

3. Parallel spin- j representation

For the parallel endpoint we use the notation of Sec. VIII: the two-spin signal is equivalent to the spin- J coherent state with $J = 2j$ and fiducial vector $|J, J\rangle$. Starting from Eq. (117), the J_z -basis matrix elements are

$$\langle J, m | Q_J^\parallel | J, m' \rangle = \int d\bar{n} p_J(n_z) D_{mJ}^{(J)}(g^{-1}) D_{Jm'}^{(J)}(g). \quad (\text{B12})$$

Since the likelihood $p_J(n_z)$ in Eq. (115) depends only on the polar angle, the azimuthal integration gives

$$\langle J, m | Q_J^\parallel | J, m' \rangle = \delta_{mm'} q_m^\parallel. \quad (\text{B13})$$

Using the standard expression for reduced Wigner matrices [61]

$$|d_{mJ}^J(\theta)|^2 = \binom{2J}{J+m} \left(\frac{1+\cos\theta}{2}\right)^{J+m} \left(\frac{1-\cos\theta}{2}\right)^{J-m}, \quad (\text{B14})$$

one obtains

$$q_m^\parallel = (2J+1) \binom{2J}{J+m} \int_{-1}^1 \frac{dx}{2} \left(\frac{1+x}{2}\right)^{3J+m} \left(\frac{1-x}{2}\right)^{J-m}. \quad (\text{B15})$$

The beta integral gives

$$q_m^\parallel = (2J+1) \binom{2J}{J+m} \frac{(3J+m)!(J-m)!}{(4J+1)!}. \quad (\text{B16})$$

Furthermore,

$$\frac{q_{m+1}^\parallel}{q_m^\parallel} = \frac{3J+m+1}{J+m+1} \geq 1, \quad (\text{B17})$$

so the largest eigenvalue is attained at $m = J$. Hence

$$F(I_{\max}^{\parallel,j}) = q_J^\parallel = \frac{2J+1}{4J+1}, \quad D(I_{\max}^{\parallel,j}) = \frac{2J}{4J+1}, \quad (\text{B18})$$

in agreement with Eqs. (119) and (120). For two parallel spin-1/2 particles, $J = 1$ and

$$Q_{J=1}^\parallel = \text{diag} \left(\frac{1}{10}, \frac{3}{10}, \frac{3}{5} \right) \quad (\text{B19})$$

in the ordered basis $\{|1, -1\rangle, |1, 0\rangle, |1, 1\rangle\}$.

Appendix C: Rank-one optimality from a one-dimensional dual kernel

We first record a sufficient condition for rank-one optimality of the covariant Choi seed. The general low-rank guarantee is proved in Appendix D; the present result identifies the common case in which the optimal seed is actually rank one.

Use the notation of Sec. VII: the sector constraints are

$$\text{Tr}(A_\ell R_0) = d_\ell, \quad d_\ell = 2\ell + 1, \quad \ell = 0, \dots, 2j, \quad (\text{C1})$$

and the supporting-line objective is $C_\mu = R_F^{(j)} + \mu R_I^{(j)}$. The dual slack is

$$K_\mu(\lambda) = \sum_{\ell=0}^{2j} \lambda_\ell A_\ell - C_\mu. \quad (\text{C2})$$

Let λ^* be an optimal dual point and suppose that the lowest eigenvalue of $K_\mu(\lambda^*)$ is simple. The dual constraint is active at optimum, so this eigenvalue is zero. Let $|X_\mu\rangle\rangle$ be the normalized kernel vector

$$K_\mu(\lambda^*)|X_\mu\rangle\rangle = 0, \quad \langle\langle X_\mu|X_\mu\rangle\rangle = 1. \quad (\text{C3})$$

Since the active lowest eigenvalue is assumed simple, the matrix constraint $K_\mu(\lambda) \geq 0$ is locally equivalent to the scalar constraint $k_{\min}(\lambda) = \lambda_{\min}[K_\mu(\lambda)] \geq 0$. The KKT stationarity condition for minimizing $f(\lambda) = \sum_\ell d_\ell \lambda_\ell$ under this active constraint gives $d_\ell = t \frac{\partial k_{\min}}{\partial \lambda_\ell}$ for some multiplier $t > 0$. First-order perturbation theory for a simple eigenvalue yields

$$\frac{\partial k_{\min}}{\partial \lambda_\ell} = \langle\langle X_\mu | \frac{\partial K_\mu}{\partial \lambda_\ell} | X_\mu \rangle\rangle = \langle\langle X_\mu | A_\ell | X_\mu \rangle\rangle, \quad (\text{C4})$$

and therefore

$$d_\ell = t \langle\langle X_\mu | A_\ell | X_\mu \rangle\rangle. \quad (\text{C5})$$

Summing over ℓ and using $\sum_\ell A_\ell = I$ and $\langle\langle X_\mu | X_\mu \rangle\rangle = 1$ gives $t = \sum_\ell d_\ell = (2j+1)^2$. Hence

$$\langle\langle X_\mu | A_\ell | X_\mu \rangle\rangle = \frac{2\ell+1}{(2j+1)^2}, \quad \ell = 0, \dots, 2j. \quad (\text{C6})$$

Therefore

$$R_0^*(\mu) = (2j+1)^2 |X_\mu\rangle\rangle \langle\langle X_\mu| \quad (\text{C7})$$

satisfies all sector constraints in Eq. (C1). Moreover $K_\mu(\lambda^*)R_0^* = 0$, so complementary slackness holds; Eq. (C7) is therefore optimal.

If the zero eigenspace is degenerate, the same reasoning gives a subgradient condition rather than a single eigenvector condition. The required sector weight vector then lies in the convex hull generated by projectors onto the active kernel. This guarantees an optimal seed of the form Eq. (57), but not necessarily a single kernel vector with the weights in Eq. (C6). Rank-one optimality in a degenerate active kernel is therefore a reduced kernel-feasibility question.

Numerically, all higher-spin branches tested in this work up to $j = 5$ have a one-dimensional active kernel in the axially symmetric block. Whenever this occurs, Eq. (C6) follows automatically from stationarity, so the sector-weight check is a consequence of the dual certificate rather than an independent fit.

Appendix D: Rank bound for optimal covariant Choi seeds

We now prove a complementary rank-reduction bound that does not assume a one-dimensional dual kernel. It uses only positivity and the number of independent sector-normalization constraints.

Consider the feasible set defined by Eq. (C1). It is compact because

$$\sum_{\ell=0}^{2j} A_\ell = I_{\text{in}} \otimes I_{\text{out}}, \quad \text{Tr } R_0 = \sum_{\ell=0}^{2j} d_\ell = (2j+1)^2. \quad (\text{D1})$$

Hence a linear supporting-line objective has an optimal extreme point. Let R_0 be such an extreme point, let $r = \text{rank } R_0$, and let P project onto its support. The real vector space $\mathcal{H}_P = \{H = H^\dagger : H = PHP\}$ has dimension r^2 . The linear map

$$\mathcal{L} : \mathcal{H}_P \longrightarrow \mathbb{R}^{2j+1}, \quad \mathcal{L}(H)_\ell = \text{Tr}(A_\ell H) \quad (\text{D2})$$

has a nonzero kernel if $r^2 > 2j+1$. A nonzero H in this kernel obeys

$$\text{Tr}(A_\ell H) = 0, \quad \ell = 0, \dots, 2j. \quad (\text{D3})$$

Since H is supported on the support of R_0 , the operators $R_0 \pm \epsilon H$ remain positive for sufficiently small $\epsilon > 0$ and, by Eq. (D3), satisfy all sector constraints. This would express R_0 as a nontrivial convex combination of two feasible points, contradicting extremality. Therefore every extreme feasible point satisfies

$$r^2 \leq 2j+1. \quad (\text{D4})$$

Consequently, for every μ there exists an optimal antiparallel Choi seed with

$$\text{rank } R_0^* \leq \lfloor \sqrt{2j+1} \rfloor. \quad (\text{D5})$$

Thus this bound forces rank one for $j = 1/2$ and $j = 1$, while for $j \geq 3/2$ it gives only low-rank existence. The one-dimensional-kernel criterion of Appendix C explains when the optimal seed can nevertheless be chosen rank one.

For the parallel benchmark the representation is irreducible. There is only one constraint, $\text{Tr } R_0 = 2J + 1$, so the feasible set is a scaled density-matrix set and its extreme points are rank-one projectors. Hence the parallel-spin tradeoff always admits an optimal seed

$$R_0^{\parallel}(\mu) = (2J + 1)|\chi_\mu\rangle\rangle\langle\langle\chi_\mu|, \quad (\text{D6})$$

where $|\chi_\mu\rangle\rangle$ is a largest-eigenvalue vector of $R_F^{\parallel} + \mu R_I^{\parallel}$.

Appendix E: Large-spin asymptotics of the antiparallel endpoint

This appendix derives the large- j limit of the maximum-information endpoint disturbance for antiparallel spin-coherent pairs. The starting point is the finite block formula in Eq. (113). We set $N = 2j$ and take the joint scaling limit

$$\ell = \sqrt{N} s, \quad \ell' = \sqrt{N} t, \quad \theta = \frac{u}{\sqrt{N}}, \quad (\text{E1})$$

with s, t, u fixed as $N \rightarrow \infty$. This is the relevant scaling because the maximum-information likelihood becomes concentrated in an angular region of width $N^{-1/2}$ around the true direction, while the Clebsch–Gordan weights in Eq. (95) are concentrated on angular momenta of order \sqrt{N} .

First, the factorial expression in Eq. (95) gives, by Stirling expansion,

$$c_\ell^2 = (2\ell + 1) \frac{(N!)^2}{(N - \ell)!(N + \ell + 1)!} \sim \frac{2s}{\sqrt{N}} e^{-s^2}, \quad (\text{E2})$$

and therefore

$$c_\ell c_{\ell'} \sim \frac{2\sqrt{st}}{\sqrt{N}} \exp\left[-\frac{s^2 + t^2}{2}\right]. \quad (\text{E3})$$

The Legendre polynomial and Wigner d -matrix elements have the standard Bessel limits [65, 66]

$$P_\ell\left(\cos \frac{u}{\sqrt{N}}\right) \simeq J_0(su), \quad d_{m0}^\ell\left(\frac{u}{\sqrt{N}}\right) \simeq (-1)^m J_m(su), \quad (\text{E4})$$

for fixed m . Using Eq. (E2), the endpoint amplitude T_j in Eq. (104) satisfies

$$T_j\left(\cos \frac{u}{\sqrt{N}}\right) \sim \sqrt{N} \int_0^\infty 2s e^{-s^2/2} J_0(su) ds = 2\sqrt{N} e^{-u^2/2}, \quad (\text{E5})$$

where the last equality follows from the Hankel transform of a Gaussian. Moreover, since $x = \cos \theta$,

$$\frac{dx}{2} \simeq \frac{u du}{2N}. \quad (\text{E6})$$

Substitution of Eqs. (E3)–(E6) into Eq. (113) gives

$$\left[Q_j^{(m)}\right]_{\ell\ell'} \sim \frac{1}{\sqrt{N}} K_m(s, t), \quad s = \frac{\ell}{\sqrt{N}}, \quad t = \frac{\ell'}{\sqrt{N}}, \quad (\text{E7})$$

where

$$\begin{aligned} K_m(s, t) &= 2\sqrt{st} \exp\left[-\frac{s^2 + t^2}{2}\right] 2 \int_0^\infty u e^{-u^2} J_m(su) J_m(tu) du \\ &= 2\sqrt{st} \exp\left[-\frac{3}{4}(s^2 + t^2)\right] I_m\left(\frac{st}{2}\right). \end{aligned} \quad (\text{E8})$$

In the second line we used a standard integral for Bessel functions [65, 67]. The finite-dimensional eigenvalue equation for $Q_j^{(m)}$ therefore converges to the integral equation

$$\int_0^\infty K_m(s, t) f(t) dt = \lambda f(s). \quad (\text{E9})$$

It remains to diagonalize the kernel. Put $x = s^2$ and write $f(s) = x^{1/4} \phi(x)$. Equation (E9) is then equivalent to

$$\int_0^\infty L_m(x, y) \phi(y) dy = \lambda \phi(x), \quad (\text{E10})$$

with

$$L_m(x, y) = \exp\left[-\frac{3}{4}(x+y)\right] I_m\left(\frac{\sqrt{xy}}{2}\right). \quad (\text{E11})$$

We diagonalize this kernel by using the generating formula for Laguerre polynomials [62, 66]. In the form needed here, for $0 < \zeta < 1$ and $\alpha > -1$,

$$\begin{aligned} & \sum_{n=0}^{\infty} \frac{n!}{\Gamma(n+\alpha+1)} L_n^{(\alpha)}(X) L_n^{(\alpha)}(Y) \zeta^n \\ &= \frac{1}{1-\zeta} \exp\left[-\frac{\zeta(X+Y)}{1-\zeta}\right] (XY\zeta)^{-\alpha/2} I_\alpha\left(\frac{2\sqrt{XY\zeta}}{1-\zeta}\right). \end{aligned} \quad (\text{E12})$$

We apply Eq. (E12) with

$$\alpha = m, \quad X = \beta x, \quad Y = \beta y.$$

Define the normalized Laguerre functions

$$\Phi_n^{(m)}(x) = \left(\frac{\beta^{m+1} n!}{\Gamma(n+m+1)}\right)^{1/2} x^{m/2} e^{-\beta x/2} L_n^{(m)}(\beta x). \quad (\text{E13})$$

Then Eq. (E12) gives

$$\sum_{n=0}^{\infty} \zeta^n \Phi_n^{(m)}(x) \Phi_n^{(m)}(y) = \frac{\beta}{1-\zeta} \zeta^{-m/2} \exp\left[-\frac{\beta(1+\zeta)}{2(1-\zeta)}(x+y)\right] I_m\left(\frac{2\beta\sqrt{\zeta xy}}{1-\zeta}\right). \quad (\text{E14})$$

We now match Eq. (E14) with the kernel $L_m(x, y)$ in Eq. (E11). This requires

$$\frac{\beta(1+\zeta)}{2(1-\zeta)} = \frac{3}{4}, \quad \frac{2\beta\sqrt{\zeta}}{1-\zeta} = \frac{1}{2}. \quad (\text{E15})$$

The solution with $0 < \zeta < 1$ is

$$\beta = \sqrt{2}, \quad \zeta = 17 - 12\sqrt{2}. \quad (\text{E16})$$

Therefore

$$L_m(x, y) = \frac{1-\zeta}{\beta} \zeta^{m/2} \sum_{n=0}^{\infty} \zeta^n \Phi_n^{(m)}(x) \Phi_n^{(m)}(y). \quad (\text{E17})$$

The eigenvalues of the integral operator are consequently

$$\lambda_n^{(m)} = \frac{1-\zeta}{\beta} \zeta^{m/2+n}. \quad (\text{E18})$$

The largest eigenvalue is obtained for $m = 0$ and $n = 0$:

$$\lambda_{\max} = 12 - 8\sqrt{2}. \quad (\text{E19})$$

Consequently,

$$\lim_{j \rightarrow \infty} F(I_{\max}^{\text{anti},j}) = 12 - 8\sqrt{2}, \quad \lim_{j \rightarrow \infty} D(I_{\max}^{\text{anti},j}) = 8\sqrt{2} - 11. \quad (\text{E20})$$

-
- [1] W. Heisenberg, Über den anschaulichen Inhalt der quantentheoretischen Kinematik und Mechanik, *Z. Phys.* **43**, 172 (1927).
- [2] C. W. Helstrom, *Quantum Detection and Estimation Theory* (Academic Press, New York, 1976).
- [3] C. A. Fuchs and A. Peres, Quantum-state disturbance versus information gain: Uncertainty relations for quantum information, *Phys. Rev. A* **53**, 2038 (1996).
- [4] K. Banaszek, Fidelity balance in quantum operations, *Phys. Rev. Lett.* **86**, 1366 (2001).
- [5] K. Banaszek and I. Devetak, Fidelity trade-off for finite ensembles of identically prepared qubits, *Phys. Rev. A* **64**, 052307 (2001).
- [6] C. A. Fuchs and K. Jacobs, Information-tradeoff relations for finite-strength quantum measurements, *Phys. Rev. A* **63**, 062305 (2001).
- [7] M. Ozawa, Uncertainty relations for noise and disturbance in generalized quantum measurements, *Ann. Phys.* **311**, 350 (2004).
- [8] L. Mišta Jr., J. Fiurášek, and R. Filip, Optimal partial estimation of multiple phases, *Phys. Rev. A* **72**, 012311 (2005).
- [9] U. L. Andersen, M. Sabuncu, R. Filip, and G. Leuchs, Experimental demonstration of coherent state estimation with minimal disturbance, *Phys. Rev. Lett.* **96**, 020409 (2006).
- [10] M. F. Sacchi, Information-disturbance tradeoff in estimating a maximally entangled state, *Phys. Rev. Lett.* **96**, 220502 (2006).
- [11] F. Buscemi and M. F. Sacchi, Information-disturbance trade-off in quantum-state discrimination, *Phys. Rev. A* **74**, 052320 (2006).
- [12] M. F. Sacchi, Information-disturbance tradeoff for spin coherent state estimation, *Phys. Rev. A* **75**, 012306 (2007).
- [13] S.-W. Lee, J. Kim, and H. Nha, Complete information balance in quantum measurement, *Quantum* **5**, 414 (2021).
- [14] S. Hong, Y.-S. Kim, Y.-W. Cho, J. Kim, S.-W. Lee, and H.-T. Lim, Demonstration of complete information trade-off in quantum measurement, *Phys. Rev. Lett.* **128**, 050401 (2022).
- [15] N. Saberian, S. J. Akhtarshenas, and F. Shahbeigi, Measurement sharpness and disturbance tradeoff, *Phys. Rev. A* **109**, 012201 (2024).
- [16] A. Asadian, F. Gams, and S. Sponar, Covariant correlation-disturbance relation and its experimental realization with spin-1/2 particles, *Phys. Rev. Research* **8**, L012011 (2026).
- [17] A. S. Holevo, *Probabilistic and Statistical Aspects of Quantum Theory* (North-Holland, Amsterdam, 1982; Edizioni della Normale, Pisa, 2011).
- [18] S. Massar and S. Popescu, Optimal extraction of information from finite quantum ensembles, *Phys. Rev. Lett.* **74**, 1259 (1995).
- [19] R. Derka, V. Bužek, and A. K. Ekert, Universal algorithm for optimal estimation of quantum states from finite ensembles via realizable generalized measurement, *Phys. Rev. Lett.* **80**, 1571 (1998).
- [20] J. I. Latorre, P. Pascual, and R. Tarrach, Minimal optimal generalized quantum measurements, *Phys. Rev. Lett.* **81**, 1351 (1998).
- [21] N. Gisin and S. Popescu, Spin flips and quantum information for antiparallel spins, *Phys. Rev. Lett.* **83**, 432 (1999).
- [22] A. Peres and P. F. Scudo, Entangled quantum states as direction indicators, *Phys. Rev. Lett.* **86**, 4160 (2001).
- [23] E. Bagan, M. Baig, and R. Muñoz-Tapia, Aligning reference frames with quantum states, *Phys. Rev. Lett.* **87**, 257903 (2001).
- [24] S. Zhang, X. Zou, C. Li, C. Jin, and G. Guo, Information–disturbance tradeoff in sending direction information via antiparallel quantum spin, *J. Phys. A: Math. Theor.* **43**, 235301 (2010).
- [25] A. Peres and W. K. Wootters, Optimal detection of quantum information, *Phys. Rev. Lett.* **66**, 1119 (1991).
- [26] S. D. Bartlett, T. Rudolph, and R. W. Spekkens, Decoherence-full subsystems and the cryptographic power of a private shared reference frame, *Phys. Rev. A* **70**, 032307 (2004).
- [27] G. Chiribella, G. M. D’Ariano, P. Perinotti, and M. F. Sacchi, Efficient use of quantum resources for the transmission of a reference frame, *Phys. Rev. Lett.* **93**, 180503 (2004).
- [28] G. Chiribella, G. M. D’Ariano, and M. F. Sacchi, Optimal estimation of group transformations using entanglement, *Phys. Rev. A* **72**, 042338 (2005).
- [29] G. Chiribella, G. M. D’Ariano, P. Perinotti, and M. F. Sacchi, Covariant quantum measurements that maximize the likelihood, *Phys. Rev. A* **70**, 062105 (2004).
- [30] G. Chiribella, L. Maccone, and P. Perinotti, Secret quantum communication of a reference frame, *Phys. Rev. Lett.* **98**, 120501 (2007).
- [31] J.-F. Tang, Z. Hou, J. Shang, H. Zhu, G.-Y. Xiang, C.-F. Li, and G.-C. Guo, Experimental optimal orienteering via parallel and antiparallel spins, *Phys. Rev. Lett.* **124**, 060502 (2020).
- [32] R. K. Patra, K. Agarwal, B. Paul, S. Roy Chowdhury, S. G. Naik, and M. Banik, Quantum incompatibility in parallel versus antiparallel spins, *Phys. Rev. Lett.* **136**, 110402 (2026).
- [33] S. Boyd and L. Vandenberghe, *Convex Optimization* (Cambridge University Press, Cambridge, 2004).

- [34] J. Watrous, *The Theory of Quantum Information* (Cambridge University Press, Cambridge, 2018).
- [35] M. Hayashi, *Group Representation for Quantum Theory* (Springer, Cham, 2017).
- [36] E. B. Davies and J. T. Lewis, An operational approach to quantum probability, *Commun. Math. Phys.* **17**, 239 (1970).
- [37] E. B. Davies, *Quantum Theory of Open Systems* (Academic Press, London, 1976).
- [38] M. Ozawa, Quantum measuring processes of continuous observables, *J. Math. Phys.* **25**, 79 (1984).
- [39] A. S. Holevo, Covariant measurements and imprimitivity systems, in *Quantum Probability and Applications to the Quantum Theory of Irreversible Processes*, Lecture Notes in Mathematics Vol. 1055, edited by L. Accardi, A. Frigerio, and V. Gorini (Springer, Berlin, 1984), pp. 153–172.
- [40] A. S. Holevo, Covariant measurements and uncertainty relations, in *Quantum Communication, Computing, and Measurement*, edited by O. Hirota, A. S. Holevo, and C. M. Caves (Plenum, New York, 1997), pp. 223–232.
- [41] K. Kraus, *States, Effects, and Operations* (Springer-Verlag, Berlin, 1983).
- [42] A. Jamiolkowski, Linear transformations which preserve trace and positive semidefiniteness of operators, *Rep. Math. Phys.* **3**, 275 (1972).
- [43] M.-D. Choi, Completely positive linear maps on complex matrices, *Linear Algebra Appl.* **10**, 285 (1975).
- [44] C. Carmeli, T. Heinosaari, and A. Toigo, Covariant quantum instruments, *J. Funct. Anal.* **257**, 3353 (2009).
- [45] G. M. D’Ariano, P. Lo Presti, and M. F. Sacchi, Bell measurements and observables, *Phys. Lett. A* **272**, 32 (2000).
- [46] F. Buscemi, G. M. D’Ariano, P. Perinotti, and M. F. Sacchi, Optimal realization of the transposition maps, *Phys. Lett. A* **314**, 374 (2003).
- [47] E. Bagan, M. Baig, A. Brey, R. Muñoz-Tapia, and R. Tarrach, Optimal encoding and decoding of a spin direction, *Phys. Rev. A* **63**, 052309 (2001).
- [48] S. Popescu, A. B. Sainz, A. J. Short, and A. Winter, Quantum reference frames and their applications to thermodynamics, *Philos. Trans. R. Soc. A* **376**, 20180111 (2018).
- [49] S. Popescu, A. B. Sainz, A. J. Short, and A. Winter, Reference frames which separately store noncommuting conserved quantities, *Phys. Rev. Lett.* **125**, 090601 (2020).
- [50] P. Hayden, S. Nezami, S. Popescu, and G. Salton, Error correction of quantum reference frame information, *PRX Quantum* **2**, 010326 (2021).
- [51] S. Zhou, Z.-W. Liu, and L. Jiang, New perspectives on covariant quantum error correction, *Quantum* **5**, 521 (2021).
- [52] Y. Yang, Y. Mo, J. M. Renes, G. Chiribella, and M. P. Woods, Optimal universal quantum error correction via bounded reference frames, *Phys. Rev. Research* **4**, 023107 (2022).
- [53] L. Kong and Z.-W. Liu, Near-optimal covariant quantum error-correcting codes from random unitaries with symmetries, *PRX Quantum* **3**, 020314 (2022).
- [54] I. Marvian, Restrictions on realizable unitary operations imposed by symmetry and locality, *Nat. Phys.* **18**, 283 (2022).
- [55] Z.-W. Liu and S. Zhou, Approximate symmetries and quantum error correction, *npj Quantum Inf.* **9**, 119 (2023).
- [56] I. Marvian, H. Liu, and A. Hulse, Rotationally invariant circuits: Universality with the exchange interaction and two ancilla qubits, *Phys. Rev. Lett.* **132**, 130201 (2024).
- [57] Although this issue does not arise in the present analysis, equivalent irreducible components cannot in general be ignored. They can be relevant for ultimate optimizations, for example in reference-frame transmission [27] or squeezing estimation [58].
- [58] G. Chiribella, G. M. D’Ariano, and M. F. Sacchi, Optimal estimation of squeezing, *Phys. Rev. A* **73**, 062103 (2006).
- [59] A. Perelomov, *Generalized Coherent States and Their Applications* (Springer-Verlag, Berlin, 1986).
- [60] F. T. Arecchi, E. Courtens, R. Gilmore, and H. Thomas, Atomic coherent states in quantum optics, *Phys. Rev. A* **6**, 2211 (1972).
- [61] A. R. Edmonds, *Angular Momentum in Quantum Mechanics* (Princeton University Press, Princeton, 1957).
- [62] G. Szegő, *Orthogonal Polynomials*, 4th ed. (American Mathematical Society, Providence, RI, 1975).
- [63] T. Kato, *Perturbation Theory for Linear Operators* (Springer, Berlin, 1995).
- [64] G. Chiribella, G. M. D’Ariano, and M. F. Sacchi, Optimal estimation of group transformations using entanglement, *Phys. Rev. A* **72**, 042338 (2005).
- [65] G. N. Watson, *A Treatise on the Theory of Bessel Functions*, 2nd ed. (Cambridge University Press, Cambridge, 1944).
- [66] F. W. J. Olver, D. W. Lozier, R. F. Boisvert, and C. W. Clark, eds., *NIST Handbook of Mathematical Functions* (Cambridge University Press, Cambridge, 2010).
- [67] I. S. Gradshteyn and I. M. Ryzhik, *Table of Integrals, Series, and Products*, 8th ed., edited by D. Zwillinger and V. Moll (Academic Press, Amsterdam, 2014).